University of South Bohemia

Faculty of Science

Localization of Lyme disease spirochetes *Borrelia burgdorferi* in ticks *Ixodes ricinus*

MASTER THESIS

Bc. Martin Strnad, BSc.

Supervisor: **RNDr. Marie Vancová, PhD**

Fuculty guarantee: **Prof. RNDr. Libor Grubhoffer, CSc.**

České Budějovice, 2013

Strnad, M., 2013: Localization of Lyme disease spirochetes *Borrelia burgdorferi* in ticks *Ixodes ricinus*. Mgr. Thesis, in English – 59 p., Faculty of Science, University of South Bohemia, České Budějovice, Czech Republic.

Annotation:

Lyme disease is the most common vector-borne infection in the Western world with an annual incidence usually in excess of 100 cases per 100 000 people in temperate areas of the United States and Europe. Same as other infectious diseases, Lyme borreliosis wreaks havoc on the host they have invaded.

B. burgdorferi, the causative agent of this disease, circulates among wildlife vertebrate hosts and *Ixodes* tick vectors but may sometimes infect humans. Its natural enzootic cycle usually occurs as follows: The larval/nymphal stage tick feeds on an infected host. During this engorgement, the spirochetes reach the tick gut and stay confined to it. After the tick molts into the next developmental stage, it finds a second host. The new bloodmeal triggers the spirochetes to multiply within the gut and traverse the gut endothelium in a highly organized manner. They finally disseminate through the hemocoel up to the tick salivary glands and into the new host. We studied whether *B. burgdorferi* is capable of reaching the tick salivary glands during the first infective feeding period in uninfected ticks.

Financial sources:

This work was conducted with institutional support RVO:60077344 from Biology Centre, Institute of Parasitology and supported by the grant from Technology Agency of the Czech Republic (TE01020118).

Declaration:

I hereby declare that I have worked on my master thesis independently and used only the sources listed in the bibliography.

I hereby declare that, in accordance with Article 47b of Act No. 111/1998 in the validwording, I agree with the publication of my master thesis, in full to be kept in the Faculty of Science archive, in electronic form in publicly accessible part of the STAG database operated by the University of South Bohemia in České Budějovice accessible through its web pages. Further, I agree to the electronic publication of the comments of my supervisor and thesis opponents and the record of the proceedings and results of the thesis defense in accordance with aforementioned Act No. 111/1998. I also agree to the comparison of the text of my thesis with the Theses.cz thesis database operated by the National Registry of University Theses and a plagiarism detection system.

Date:

Signature:

ACKNOWLEDGEMENTS

I would like to express my gratitude to my supervisor, Marie Vancová, whose expertise and patience helped me fundamentally throughout my studies and my research. I want to thank all the employees at the laboratory of electron microscopy for making me feel welcome and providing guidance when needed. Further, I would like thank Ryan Rego for the critical proofreading of the thesis and for his essential advice regarding the molecular biology. Many thanks go to Prof Libor Grubhoffer, whose kindness made me feel positive during all the exacting study days. I would also like to thank my teammates from the football club SK Nemanice, who are always able to boost my mood. Last but not least, I want to thank my family and my girlfriend Lenka for all their help and support throughout my six years as a student.

LIST OF ABBREVIATIONS

CLEM - correlative light electron microscopy

EM - electron microscopy

FlaB - flagellin B protein

FITC - fluorescein isothiocyanate

FLM- fluorescence light microscopy

OspA/C - outer surface protein A or C

PFs - periplasmic flagella

PBS - phosphate buffer saline

PB - phosphate buffer

RT - room temperature

QDs - quantum dots

SGs - salivary glands

SEM - scanning electron microscopy

TAE - tris acetate-EDTA

TEM - transmission electron microscopy

TRITC - tetramethyl rhodamine isothiocyanate

TABLE OF CONTENTS

1 INTRODUCTION

1.1 Lyme Disease

Lyme disease, or Lyme borreliosis, is the most common vector-borne infection in the Western world with annual incidence exceeding the boundary of 100 cases per 100 000 people in temperate areas of the United States and Europe (Bacon *et al*., 2008). If not recognized or treated appropriately, Lyme borreliosis might lead to a wide array of complications. The symptoms of Lyme disease vary, but share some common features such as flu-like illness and erythema chronicum migrans (skin rash). Afterwards, symptoms like arthritis, skin disorders and various neurological complications may occur (Barbour *et al*., 1983). Lyme borreliosis was first recognized when statistically unlikely cluster of juvenile rheumatoid arthritis appeared in 1975 in Old Lyme, Connecticut (USA). After intense clinical and epidemiologic research, it became apparent that the arthritis was a late manifestation of a tick-transmitted illness. Two years later, Lyme disease was finally reported as an infectious disease by Steere (Steere *et al*., 1977). The causative agent of the disease, a spirochete-like bacteria, was identified in the early 1980s by medical entomologist Willy Burgdorfer and subsequently named in his honor - *Borrelia burgdorferi*. Nevertheless, it lasted more than three decades after Burgdorfer's discovery to find out that the causative agent is part of a wider grouping of spirochetes known as *Borrelia burgdorferi* sensu lato (Hovius *et al*., 2007). *Borrelia burgdorferi* sensu lato complex comprises 18 named spirochete species, out of which 3 commonly and 4 occasionally infect humans (Rudenko *et al*., 2011).

1.1.1 *B. burgdorferi* anatomy and genomic organisation

Borrelia burgdorferi is a pathogenic organism that is capable of colonizing a wide array of animals, i.e. arthropods, birds, or mammals. It is a typical representative of spirochete-like bacteria, usually 20-30 µm long and 0.2-0.5 µm wide (Barbour and Hayes, 1986). *B. burgdorferi* have a protoplasmic cell cylinder which includes the plasma membrane and peptidoglycan layer, and an outer membrane (Figure 1). The region between the peptidoglycan layer and the outer membrane forms the periplasmic space. Because of its double-membrane envelope, *B. burgdorferi* are often mistakenly classified among Gram negative bacteria. The lack of lipopolysaccharides and the presence of major surface

lipoproteins is what distinguishes them markedly from Gram negative species (Samuels and Radolph, 2010a).

Motility in *B. burgdorferi* is provided by bundles of between 7 - 11 periplasmic flagella (PFs), which are anchored to motor complexes situated near the ends of the spirochete (Wolgemuth *et al*., 2006). In contrast to the majority of bacteria, the PFs do not extend out of the surface into the surroundings. Rather, the flagellar filaments are enclosed in the periplasmic space. The major constituent of PFs is a flagellin protein, FlaB. The PFs are rotated by the flagellar nanomachines, imposing on *Borrelia* the characteristic flat-wave morphology. As a consequence of its unique morphology, *B.burgdorferi* are able to pass through viscous gel-like media in which most other flagellated bacteria are not able to move (Kimsey and Spielman, 1990). When the flagellin gene *flaB* is mutated, the spirochetes lose their motility, and in addition to that, acquire a rod-shape morphology (Motaleb *et al*., 2000). It has now been shown that this loss of motility is crucial for infectivity of *B. burgdorferi* in the mouse-tick infectious cycle (Sultan *et al*., 2013). One more peculiarity of *B. burgdorferi*; it is not an alternative sigma factor σ^{28}, so typically employed in flagella biosynthesis in many other bacteria species, but rather the primary sigma factor σ^{70} that was proven to be the main regulator of the flagella synthesis and chemotaxis (Ge *et al*., 1997).

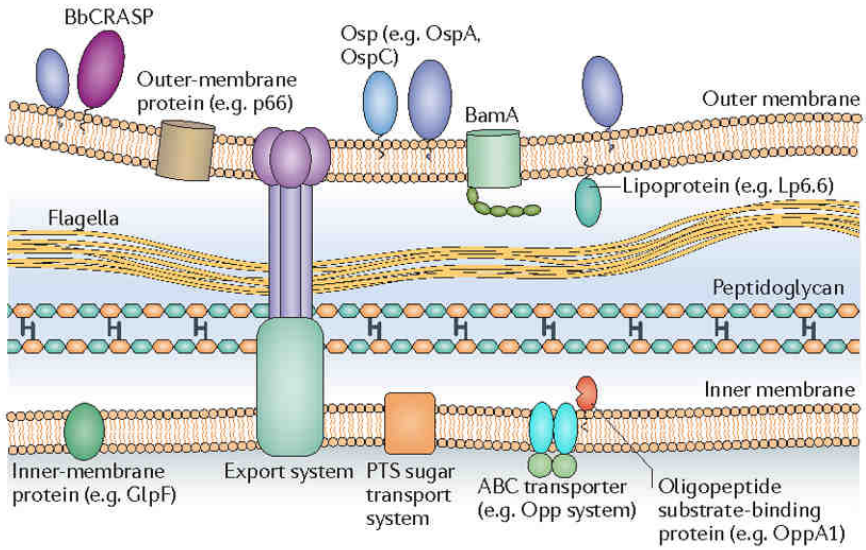

Figure 1. The schematic overview of the borrelial cell envelope. Osp, outer surface protein; BbCRASP, complement regulator-acquiring protein; BamA, β-barrel outer-membrane-spanning protein. Reproduced from Radolph *et al*. (2012).

The first complete genome sequence of *B. burgdorferi* strain 31 has been known for more than 10 years (Fraser *et al*., 1997). The linear chromosome is relatively small compared with the overwhelming majority of bacteria, including other spirochetes. It has about 950 kb in length and carries the majority of the housekeeping genes. The chromosome is fairly invariable in gene composition and organization. The modest size of the chromosome with only a minimum of genes encoding for biosynthetic and metabolic reactions is consistent with dependence on a bountiful host environment. It also implies *Borrelia in-vitro* cultivation in the laboratory being an exacting task. Genes governing cell wall synthesis; DNA, RNA and protein biosynthesis and glycolysis belong among the units of heredity encoded on the linear chromosome (Samuels and Radolph, 2010b). Although more than half of the genes found on the linear chromosome are also present within other bacterial species, the vast majority of genes encoded on plasmids (extrachromosomal genetic elements) seem to be completely unique to the *Borrelia* genus. *B. burgdorferi* isolate B31, the first sequenced *B. burgdorferi* strain, contains at least 12 linear plasmids (denoted 'lp') (lp5, lp17, lp21, lp25, lp28-1, lp28-2, lp28-3, lp28-4, lp36, lp38, lp54, and lp56) and 9 circular plasmids (denoted 'cp') (cp9, cp26, cp32-1, cp32-3, cp32-4, cp32-6, cp32-7, cp32-8, and cp32-9). This assortment of plasmids totals together about 600 kb (Fraser *et al*., 1997; Casjens *et al*., 2000). Nevertheless, the number of replicons varies between *B. burgdorferi* isolates from distinct geographic areas. At least 9 new plasmid types different from that found in the first sequenced B31 isolate were observed (Schutzer *et al*., 2011). Determining the exact figure of plasmids is often hindered by the presence of paralogous sequences on different plasmids in the same cell, thus making the plasmid identification very complicated (Casjens *et al*., 2000). Plasmid-encoded genes have been reported to be necessary for infectivity and persistence in the arthropod or the vertebrate host (see details later in 'Introduction').

B. burgdorferi strain identification is first and foremost based on nucleotide sequences of either of the *ospC* gene (coding for outer surface protein C), or the intergenic spacer 1 (IGS1) (reviewed by Travinsky *et al*., 2010). By genotyping the *ospC* gene, more than 20 specific genotypes have been defined. *OspC* locus is of special relevance as it codes for a protein that is a major surface lipoprotein produced by *B.burgdorferi* when infected ticks feed (Grimm *et al*., 2004; Pal *et al*., 2004). There are some reports endeavouring to link the disease severity and *B. burgdorferi* genotypes (Wormser *et al*., 2008; Dykhuizen *et al*.,

2008), even though typing only a single locus should not be adequate for plausible assessment and prediction of strain's virulence potential (Travinsky *et al*., 2010).

1.1.2 Transmission of spirochetes

At the onset of study of the Lyme disease, there was gentle discord among scientists about how vector ticks actually transmit this new pathogen. Burgdorfer *et al*. (1989) suggested that transmission of the spirochetes could be associated with fecal contamination or tick regurgitation. These ways of transmission became improbable after the bacteria were confirmed in the hemolymph (Benach *et al*., 1987) and salivary glands of feeding ticks (Zung *et al*., 1989). These findings demonstrated that *B. burgdorferi* spirochetes infect vertebrate hosts via a salivary gland route. Transovarial transmission has been mentioned regularly in the literature since the discovery of Lyme borreliosis. Burgdorfer *et al*. (1983) reported transovarial transmission rates of 100% and 60% of a pair of *Ixodes ricinus* females. However, new studies do not reckon this transmission pathway among well-established phenomena (Rollend *et al*., 2013). On the basis of published data (Nefedova *et al*., 2004; Lane and Burgdorfer, 1987), transovarial transmission does not seem to play any essential role in the maintenance of *Borrelia* in their enzootic cycle.

1.1.3 Transtadial transmission of spirochetes

The genus *Borrelia* is conventionally divided into two groups (families): those causing Lyme disease and those giving rise to relapsing fever. In addition to these Borrelia categories, a new group of reptile-associated *Borrelia* has been reported (Takano *et al*., 2011).

Transstadial (from one developmental stage of the vector to its subsequent stage) transmission is common within all three groups, however, the Lyme disease and reptile-associated spirochetes are primarily confined to the gut of the tick after the molt (Piesman, 1995). The dissemination from the gut to the salivary glands is initialized by attachment of the tick to a new host. Relapsing fever spirochetes are present also predominantly in the gut after the molt but further they can reach and persist in other tissues including the salivary glands (Schwan and Piesman, 2002; Takano *et al*., 2012). The consequence of this phenomenom is that relapsing fever *Borrelia* can be transmitted to a new host within minutes after attachment.

1.1.4 Spirochete multiplication

When a tick in the larval stage ingests blood containing spirochetes from an infected host, the bacteria, after reaching the gut, start multiplying vigorously. They proliferate in the replete tick until the nymphal molt, when an intense decrease in spirochete numbers occurs (Burkot *et al*., 1994). Gut immunity is probably the critical factor of tick competence. The gut lumen is a hostile milieu for ingested pathogens. It is mainly due to the antimicrobial activity of hemoglobin fragments formed during digestion of the host blood cells. Reactive oxygen species presumably also play a crucial role in tick-pathogen interactions (Kopáček *et al*., 2010). At the time, before the tick finds and attaches to a new host, the spirochetes generally lie dormant in the lumen of the gut. The new bloodmeal triggers the spirochetes to multiply within the gut and traverse the gut endothelium in a highly organized manner (Schwan and Piesman, 2002).

Dunham-Ems *et al*. (2009) demonstrated that dissemination of *B. burgdorferi* within ticks is not solely motility driven. They proposed a so-called „biphasic mode of dissemination". Herein, in the initial phase of gut evasion, the spirochetes multiply substantially and coalesce into adherent networks of non-motile individuals that slowly proceed toward the basolateral membrane while „adhering to differentiating, hypertrophying, and detaching epithelial cells." Afterwards, in the second phase, the non-motile spirochetes transition to motile phenotype that breach, via an extracellular route, the basement membrane of the gut and enter into the hemocoel. The dissemination of spirochetes is enhanced by the acquisition of plasminogen, a precursor of trypsin-like serine protease plasmin, which facilitates penetration of the basement membrane (Coleman *et al*., 1997). Once in the hemocoel, the spirochetes must contend with the mediators of tick innate immunity, hemocytes and defensins, as they traffic toward the salivary glands (Sonenshine and Hynes, 2008). The chemoattractive effect of salivary glands was shown to play a role in the navigation of the spirochetes (Shih et al., 2002), therefore, it also may contribute to transmission of the bacteria and establishment of mammalian infection (Sze et al., 2012).

1.1.5 Gene products required for infectivity and persistence during enzootic cycle

Considerable attention has been paid lately to differential gene expression by *B. burgdorferi* during the tick feeding. The products of the activated genes can be sorted out according to their roles, which they play in the process of tick and mammalian infection; either mediate interactions with the host, or compete with the host immune system, thus facilitating survival in various tissues and organs (Tilly *et al*., 2008).

B. burgdorferi spirochetes have to adapt in two totally dissimilar milieus during their enzootic cycle. When infected nymphal ticks engorge, the antigenic composition of *Borrelia* alters fundamentally. Signals that provoke the expression of a new set of proteins are believed to be rather external than internal. During the tick feeding, temperature in the tick gut raises from 23°C up to 37°C (Piesman *et al*., 2001). In addition, the pH value drops from 7.4 down to 6.8 (Yang *et al*., 2000).

The most thoroughly studied borrelial lipoprotein is outer surface protein OspA, which was shown to be abundant on the surface of spirochetes in unfed nymphal and adult ticks (Barbour *et al*., 1983). OspA serves as an adhesin to the gut cells. It enhances retention of spirochetes in the gut during off-host periods of ticks. TROSPA, a receptor for OspA binding, which mediates spirochetal attachment to gut epithelial cells, was identified (Pal *et al*., 2004b). OspA is gradually downregulated during tick feeding, allowing the bacteria to leave the gut and disseminate through hemocoel into the salivary glands.

Among the other expressed genes that facilitate the *Borrelia* survival within the tick gut belong *ospD* (Li *et al*., 2007), *bptA* (Revel *et al.*, 2005), and *ospB* (Fikrig *et al*., 2004). OspB, another surface-exposed lipoprotein, is structurally similar to OspA. In addition, both are encoded on the same linear plasmid lp54 (Fraser *et al*., 1997). A receptor molecule for OspB, however, has not been identified yet (Neelakanta *et al*., 2007). The study carried out by Neelakanta *et al*. (2007) indicates that OspB-deficient spirochetes, similarly to OspA-deficient bacteria, have impaired ability to survive in the tick gut.

Factors essential for survival of *B. burgdorferi* within a mammalian host have been under the scope of science more than those that are required for tick vector colonization. The reason for this is that these outer membrane proteins (OMPs) suggest themselves as potential vaccine candidates (Table 1). OMPs comprise a wide range proteins and their derivatives (e.g. lipoproteins), including the outer surface proteins (Osp).

Table 1. Localization and function of important *B. burgdorferi* genes.

Gene/Gene product	Gene location	Function of gene product
ospA	lp54	Tick gut adhesin
ospB	lp54	Tick gut adhesin
ospC	cp26	Tick-host transmission
dbpA	lp54	Binds decorin; host colonization
dbpB	lp54	Binds decorin; host colonization
vlsE	lp28-1	Enhances borrelial immune evasion
bbk32	lp36	Binds fibronectin; host colonization
p66	chromosome	Binds integrin; host colonization
erpP, *erpA*, *erpC*	cp32	Inactivation of the host complement pathway

(Reviewed by Singh and Girschick, 2004)

Schwan *et al*. (1995) described a reciprocal expression of the genes encoding OspA and OspC during the transmission cycle of spirochetes. While OspA is downregulated during tick feeding, *ospC* gene is activated. OspC is much more polymorphic than OspA (Nordstrand *et al*., 2000). Its diversity may be caused by various mechanisms, including host-stimulated immunological selection, intragenomic recombination, and changes in environmental conditions. Of these factors, immunological pressure is probably the striking force in maintaining the variation of OspC (Wang *et al*., 1999).

The opinions on OspC diverge with regard to its function. It has been shown that OspC production is distinctively upregulated during transmission from the tick vector to the mammalian host (De Silva and Fikrig, 1995). Therefore, OspC might be engaged in escaping from the gut, invading the salivary glands, and/or establishing the mammalian infection. Though the sphere of activity of OspC has been studied in many laboratories, no unanimous verdict on its impact has been truly accepted.

Among the first works touching population dynamics of OspC and OspA during *Borrelia* dissemination from the ticks gut to mice belongs the study carried out by Ohnishi *et al.* (2001). He proposed that the role of OspC is only in allowing the spirochetes to leave the gut in order to reach the hemocoel. His results showed that a vast majority of spirochetes invading the tick salivary glands were neither OspC nor OspA-positive. The same holds true for spirochetes that reached the dermis of the host mice. Additionally, this work demonstrated that ticks had to be attached to mice for at least 53 hr to enable stable transmission of spirochetes into the mammalian host. The immature specimens, which invaded the mice earlier produced predominantly OspA and, moreover, were not able to establish infection.

Pal *et al.* (2004a) focused in his research on clarification of the role of OspC during the invasion of the tick salivary glands. He found out that spirochetes producing OspC were able to reach the salivary glands, but the OspC-deficient bacteria were not. Once the OspC-deficient spirochetes were complemented with plasmid containing the *ospC* gene, the settlement of the salivary glands was completely restored. These results indicate that OspC is a very important constituent enabling spirochetes to invade the tick salivary glands. Grimm *et al.* (2004) investigated the capability of *ospC* mutant to disseminate from the gut to the salivary glands during tick feeding. Her results positively correlate with the findings of Ohnishi *et al.* (2001) in a way that OspC is not required for *Borrelia* migration from the gut to the salivary glands. Another substantial observation in this study was that OspC is an essential virulence factor required during the first days of mammalian infection. These results were confirmed by Tilly *et al.* (2006 and 2009). The *ospC* gene is completely shut off after few weeks of mammalian infection (Liang *et al*., 2002). Once the spirochetes adapt to a mammalian host, they can infect and proliferate in the absence of OspC. Interestingly, constitutive expression of *ospC* has fundamentaly adverse effects on spirochetes in immunocompetent hosts (Xu *et al*., 2006). Therefore, it is hypothesized that another lipoprotein present on host-adapted spirochetes carries out the same vital function initially performed by OspC. This, until now unknown protein, substitute for OspC and is produced during the persistent infection (Tilly *et al*., 2009). Variable surface antigen VlsE, another surface-exposed lipoprotein, may be the candidate.

The biological function of VlsE has not been completely clarified yet, but there is evidence showing that VlsE is a significant virulence factor within mammalian hosts. Its pronounced antigenic variation plays an important role in *B. burgdorferi* immune evasion (Coutte *et al*., 2009). The *vls* locus consists of an expression site for the VlsE lipoprotein and 15 upstream silent cassetes which have been shown to recombine with the *vlsE* region, imposing a substantial antigenic variation so important in immune evasion (Zhang and Norris, 1998). Interestingly, VlsE and OspC share some general structural features. For instance, membrane proximal parts of both molecules form long helices (Eicken *et al*., 2002). Loss of lp28-1, plasmid containing *vlsE* coding sequence, imposed a decrease of infectivity in the mouse model (Purser and Norris, 2000).

1.1.6 Correlation between plasmids and infectivity

A considerable body of evidence proves, beyond reasonable doubt, that *B. burgdorferi* plasmids are deeply associated with pathogenesis. It is well demonstrated that *in-vitro* passage causes loss of many plasmids (Xu *et al.*, 1996; Barbour, 1998). Interestingly, the loss of cp26, which contains the *ospC* coding sequence, has never been noted in any examined isolates (Terekhova *et al*., 2006). Norris *et al.* (1995) showed that high- and low-infectivity clones exist side-by-side within a population, but plasmid-deficient (low-infectivity) subclones prevail in higher (>15) *in-vitro* passages. The plasmid content differs even within the three most pathogenic strains for humans; *B. burgdorferi* sensu stricto, *B. garinii,* and *B. afzelii (Purser and Norris, 2000).*

Some of the plasmids, which are undisputedly connected with pathogenesis and infectivity in the mammalian host and, to a lesser extent, in the tick vector have been already identified. For instance, lp25, lp28-1, lp36, lp54 and cp26 were proven to exhibit a direct correlation with persistent infection within mice (*Purser and Norris, 2000; Labandeira-Rey and Skare, 2001; Jewett et al., 2007; Hagman et al., 1998*). The plasmids being reported to take part in the establishment of infection and dissemination within the tick vector include lp25, lp54, and cp26 (Grimm *et al*., 2005; Yang *et al*., 2004; Pal *et al*., 2004a). However, the studies claiming that cp26 or, strictly speaking, cp26-encoded *ospC* gene is not required for migration from the tick's gut to the SGs decidedly outnumber the studies that state otherwise.

1.1.7 Indispensable gene products for mammalian infection

Early studies have demonstrated that the foremost virulence factors participating in establishment of vertebrate infection are present on the linear plasmids 25 and 28-1. The enzyme (encoded on lp25) shown to be essential for borrelial survival, and a key infectivity determinant in a mammalian host, is nicotinamidase (PncA), involved in NAD production (Purser *et al*., 2003). The mystery of lp28-1 determinant has not been unravelled yet, but the surface exposed lipoprotein VlsE is the likely candidate. The bacteria lacking lp25 are considered to be noninfectious, while those missing lp28-1 are deemed low- or intermediate-infectious. For maximal infectivity both must be present. The lp28-1-deficient *Borrelia* are able to invade various mammalian tissues such as skin, bladder, and/or joint cells but are capable of maintaining only in the joints (*Labandeira-Rey and Skare, 2003*).

1.2 Ticks

Ticks are obligate hematophagous parasites of reptiles, birds and mammals. The order *Ixodida* include three families; the *Ixodidae*, the *Argasidae* and the *Nuttalliellidae* (Hoogstraal, 1985). The majority of hard ticks (*Ixodidae*) are known as three-host ticks, each tick developmental stage (larvae, nymph, adult) feeds on a different host (Figure 2). The principal (competent) tick vector of Lyme borreliosis spirochetes in Europe is *Ixodes ricinus* which is found mainly in cool humid environments (e.g. forests). *I. ricinus* transmits a broad range of bacterial pathogens to humans, including *Borrelia burgdorferi*, *Babesia bigemina* and *Anaplasma phagocitophylum*. In addition, tick-borne encephalitis, a viral infection of the central nervous system, is spread by this tick species (Estrada-Pena *et al*., 2004).

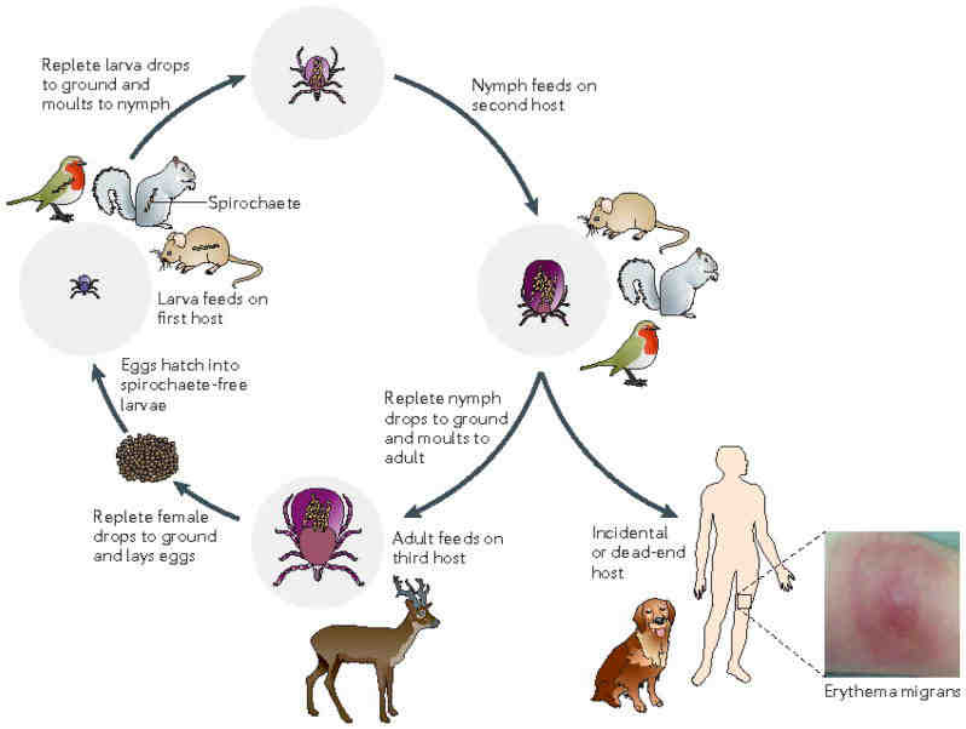

Figure 2. A three-stage life cycle of *Ixodes* ticks. Each life stage with a different host. Reproduced from Radolph *et al*. (2012).

1.2.1 Salivary glands of ixodid ticks

Salivary glands of ixodid ticks are paired structures that fill up approximately the anterior one-third of the tick's hemocoel. They are consisted of three types of acini, one agranular (type I acini) and two granular (type II and III acini). The salivary excretions released into the feeding site influence the host immune system and hemostasis. Moreover, salivary glands play a vital role in osmoregulation (Amoreaux *et al*., 2003). The type I acini are located closest to the tick mouthpart, draining directly into the main salivary duct. Acinus I is responsible for secretion of a hyperosmotic (very salty) fluid facilititating the water uptake when the tick is off its host. Type II and III acini produce a wide array of bioactive proteins and lipids, acting as immunosuppressants and anticoagulants during tick feeding. Unlike acinus I, acini II and III enlarge markedly during feeding (reviewed by Bowman and Sauer, 2004). When on-host, ticks regularly alternate blood ingestion and salivation, each period taking approximately 10 - 15 min (Francischetti *et al*., 2009). The salivary glands perform another important function; produce a cement-like substance that strengthen the attachment of the tick hypostome to the skin of its host.

Tick salivary proteins considerably affect the enzootic cycle of *B. burgdorferi*. Whether it concerns their transmission from the host to the tick vector (Narasimhan *et al*., 2007), or *vice versa*. The most interesting from the latter category is a multifunctional protein Salp15. First, Salp15 exerts immunosuppressive effects on the vertebrate host, such as inhibiting CD4+ T-cell activation (Anguita *et al*., 2002). Secondly, binding of Salp15 to OspC protects the bacteria from antibody-mediated killing by the host (Ramamoorthi *et al*., 2005; Hovius *et al*., 2008).

1.2.2 Salivary glands degeneration

The onset of degeneration in adult ticks (no literature available pertaining to nymphs to date) from a family *Ixodidae* is characterized by a decline in cells secretion, following with changes in size and shape of cells and nuclei, chromatin fragmentation, and formation and release of apoptotic bodies (Furquim *et al*., 2008). The study made by Furquim (2008) showed that the rate of degeneracy is asynchronous among acini of different types. Type I acini that are involved in off-host osmoregulation have been proven to be the least rapidly degenerating, whereas the changes in types III and IV acini (*Rhipicephalus sanguineus* has 4 types of acini) were much more prominent during first days post-detachment. In adult females, one of the triggering stimuli of degeneration is surpassing a ‘critical weight‘ (Friesen and Kaufman, 2009). Among the other stimuli belong a so-called ‘male factor‘, a set of undefined biochemical substances transmitted to females during mating (Kaufman and Lomas, 1996). Salivary glands degeneration is considerably delayed if the adult females are virgin (Friesen and Kaufman, 2009). The degeneration occurs through apoptosis rather than necrosis. The executive chemical messenger responsible for the autolytic process is ecdysteroid (Lomas *et al*., 1998). Ectysteroid is also a common insect molting hormone, which is probably the reason why many scientists believe that salivary glands degenerate during the juvenile ticks molt to such an extent that it cannot transpass the *Borrelia burgdorferi* spirochetes into the next developmental stage.

1.3 Artificial feeding of ticks

Various artificial feeding systems have been tested throughout the past few decades. The obvious question which comes up to one‘s mind is what is the advantage to feed ticks *in vitro*. Besides the ethical aspects of using experimental animals, the expenditures on rearing hosts for ticks are eminent. In addition, *in vivo* trials with animals require repetitions due to the inherent variations between individual experimental animals. That means a lot of ticks, time, and other products are frittered away (Kröber and Guerin, 2007a).

1.3.1 Short history of tick-feeding assays

The first assays for artificial tick-feeding are documented in the 1950s. At that time ticks were successfully fed upon the air sac membrane of embryonated chicken eggs (Burgdorfer and Pickens, 1954) and upon blood-filled capillary tubes positioned over the ticks’s mouthparts (Chabaud, 1950). The capillary tube feeding system was modified lately by Purnell and Joyner (1967). They allowed ticks to pre-fed on their natural animal hosts before putting them on the glass capillary tube system. The disadvantage of this system was that ticks were not capable to feed to repletion. Kemp *et al*. (1975) achieved >50% moult by engorged larvae of the cattle tick *Boophilus microplus* fed on culture medium through thin (0.3-0.5 mm) skin slices of cattle. Voluntary attachment and blood-feeding of ixodid ticks on an artificial membrane (glue-impregnated Baudruche membrane) was documented first by Waladde *et al*. (1979). The use of a silicone-impregnated membrane (Hadebank and Hiepe, 1993) and consequent implementation of elastic properties of skin into the membrane (Kröber and Guerin, 2007a) permitted higher tick attachment rates. Semi-artificial skin membrane feeding is a method of choice for tick species with shorter hypostome that are unable to completely penetrate the artificial membrane (Bonnet *et al*., 2007; Hatta *et al*., 2012).

1.4 Microscopy in cell biology

The first half of the twentieth century is related with a major explosion in the biological fields such as cell biology, molecular biology or biophysics. It was caused by the development of electron microscopy and by the improvements in the light microscopy techniques (Masters, 2009). Cell biology is an umbrella term, which encompasses the study of cell organelles, structure, reproduction, and communication with its environment.

Depending on the investigation interest and size of the studied structure, researchers can choose from a wide array of (live-) imaging methods.

1.4.1 Fluorescence light microscopy

According to the equation proposed by Ernst Abbe and Lord Rayleigh, light microscopes cannot resolve two separate entities that are closer than one-half the wavelength of light, approximately 200 - 300 nm (Abbe, 1873; Rayleigh, 1896). Their findings implied that the resolution of an image is not limited by the performance of the instrument, but only by the wavelength of light and the numerical aperture of lenses (Cortese *et al*., 2009). Since this so-called ‘diffraction limit‘ was considered a law of nature for over a century, it considerably constrained the development of optical microscopy (Gustafsson, 2008). Recently, however, the diffraction limit has been beaten by several special approaches, where the spatial resolution on the order of few tens of nanometers was achieved (Cortese *et al*., 2009).

Apart from the conventional fixed-cell imaging, so-called live-cell fluorescence microscopy has become a requisite tool in many modern cell biology laboratories. The most critical challenge for executing successful live-cell imaging experiments is to retain the biological system in a healthy state and functioning normally while being under investigation.

1.4.2 Electron microscopy

To enhance the resolving power of a light microscope either the finite aperture of lenses has to be increased, or the wavelength of the illumination has to be shortened. For EM the latter case holds true. The wavelength of electrons is usually smaller than 1 Å, depending on the accelerating voltage (Masters, 2009). EM can usually reveal cellular structures with a resolution of single nanometers. Nowadays, however, subnanometer resolution EM is not a science fiction (Serysheva *et al*., 2008).

There are several factors that hinder EM from flourishing. EM requires fixation of the studied material, resulting in static images with impossibilty of live observation (van Rijnsoever *et al*., 2008). Difficult localization of regions of interest is another drawback of EM. The time invested in locating the area of interest may sometimes exceed the time required for actual data acquisition (Kolotuev *et al*., 2009). Last but not least, electron microscopes are extremely expensive.

Several types of electron microscopes have been invented to investigate different aspects of a specimen. The two most common types are a transmission electron microscope and a scanning electron microscope. Transmission electron microscope was the first electron microscope to be developed. It can be compared with a slide projector. In TEM, the light source is replaced by an electron source, the glass lenses are replaced by (electro)magnetic lenses, and the projection screen is replaced by an imaging device such as a fluorescence screen or a CCD (charge-coupled device) camera. The sample being studied by TEM has to be thin enough to allow the electrons to penetrate it. (www.fei.com).

SEM is a method of choice if you want to look at the surface of the sample. It works by scanning the surface of the specimen with an electron beam (primary electrons) and detecting electrons that are reflected (backscattered electrons; BSE) or knocked away (secondary electrons; SE) from the sample surface. The resolving power of SEM is lower than that of TEM, roughly by an order of magnitude. Increased magnification is produced by decreasing the size of the scanned area.

One of the state-of-art devices for SEM is a field emission scanning electron microscope (FESEM JEOL 7401F). It incorporates a cold cathode field emission gun, ultra high vacuum (10^{-7} Pa), and high-tech modules for high resolution (1 nm) imaging. By using a Gentle Beam^{TM} method, this microscope yields very high resolution even at low acceleration voltage (0.1 kV) (www.speciation.net).

1.4.3 Correlative light and electron microscopy

Correlative light electron microscopy (CLEM) is a method that bridges the gap between light and electron microscopy. A limitation of fluorescence light microscopy (FLM) is that it lacks fine structural information; precise identification of unlabeled structures is impossible (van Rijnsover *et al.*, 2008). Moreover, false-positive signals caused by non-specific staining or autofluorescence cannot be ruled out. Furthemore, conventional FLM is not able to provide near-atomic-level spatial resolution. Where FLM falls short of performance, there EM hurries to help. The resolving power of the transmission microscope is about two orders of magnitude greater and, moreover, EM provides the needed reference space, where both labeled and unlabeled structures can be visually examined (Cortese *et al*., 2009). Even though the new super resolution FLM techniques have almost cleared away the resolution gap between FLM and EM, their availability still lags behing (Cortese *et al*., 2012). The

need for specific and expensive equipment and the high complexity of the protocols is what hold back the fast expansion of CLEM (Schwarz and Humbel, 2007). Nevertheless, today is CLEM one of the most intensively developing electron microscopy techniques.

The ideal CLEM probe is visible by FLM as well as by EM. These probes can be either combinatorial or possess the intrinsic properties, which allow observation at both FLM and EM (Sosinsky *et al*., 2007). In the combinatorial design, both a fluorochrome and an electron-dense gold particle are conjugated to the same antibody. In early attempts the colloidal-gold-conjugated antibodies were tested, but it was ascertained that fluorescence is quenched by colloidal gold (Powell *et al*., 1998). This issue can be overcome by using nanogold particles (e.g. FluoroNanogold^{TM}) covalently linked to the antibody fragment. The shortcoming of FluoroNanogold^{TM} is that the gold particles are only 1.4 nm in diameter, therefore, silver enhancement is necessary. Gold-conjugated antibodies aimed directly against fluorochromes were also documented (van Dam *et al*., 1991). An example of probes that possess the intrinsic properties to be detectable at both FLM and EM are luminescent semiconductor QDs, which are highly convenient for multiprotein labeling (Giepmans, 2008). The drawback of QDs is that they are small and their electron density in not as high as of the gold particles, therefore, their detection in cell cultures (especially when contrasted with uranyl acetate/lead citrate) is difficult (personal discussion with Marie Vancová). Another method for correlated microscopy exploiting the phenomenom of photoconversion. Fluorescent probes (e.g. green fluorescent protein) are able to generate highly reactive singlet oxygen species. These oxygen species can be harnessed to oxidize diaminobenzidine (DAB). The oxidized DAB forms polymers that are osmiophilic and readily detectable at EM (Sosinsky *et al*., 2007).

2 GOALS OF THE WORK

- Implementation and optimization of an *in-vitro* tick feeding method.
- Assessment of the use of an artificial silicone membrane feeding technique as a reliable tool to achieve borrelial infection in ticks.
- Attempt to challenge the conventional viewpoint that *Borrelia* can disseminate from the tick gut to the salivary glands only during “second“ feeding.
- To correlate dissemination ability of *B. burgdorferi* with plasmid content.
- Detection of *B. burgdorferi* spirochetes using correlative light electron microscopy.
- To bring new insights into the molting process of nymphal ticks and touch on the possibility of transstadial transmission of *Borrelia* inside the tick salivary glands.

3 MATERIAL

Chemicals:

Table 3. Material used for fluorescence microscopy examination.

Fluorescence Microscopy	Blocking buffer	BSA	Sigma, MO (USA)
		Nonfat-dried milk	Sigma, MO (USA)
		Glycine	Sigma, MO (USA)
	Primary IgG	rabbit anti-*Borrelia* IgG (polyclonal)	Thermo Scientific, MA (USA)
		mouse anti-OspC IgG (monoclonal, BBM45)	Baxter, Austria (from Ian *Livey*)
	Secondary IgG	(FITC)-conjugated goat anti-mouse IgG	Jackson Immuno Research Labs, PA (USA)
		(TRITC)-conjugated goat anti-rabbit IgG	
	Mounting medium (self-prepared)	polyvinylalcohol-DABCO	2.5% DABCO 10% polyvinylalcohol 5% glyrerol 25 mM Tris buffer pH 8.7

Table 4. Material used for correlative light electron microscopy examination.

Correlative Light Electron Microscopy	Cryoprotectant	2.3 M Sucrose	Sigma-Aldrich, MO (USA)
	Blocking buffer	BSA-c	Aurion, Netherlands
		Nonfat-dried milk	Sigma-Aldrich, MO (USA)
		Glycine	Sigma-Aldrich, MO (USA)
	Primary IgG	rabbit anti-*Borrelia* IgG	Thermo Scientific, MA (USA)
	Secondary IgG	(FITC)-conjugated goat anti-rabbit IgG	Jackson Immuno Research Labs, PA (USA)
	Tertiary IgG	(gold)-conjugated mouse anti-FITC IgG (MAFITC-10 nm gold)	Aurion, Netherlands
	Mounting medium	VECTASHIELD® HardSet™ Mounting Medium with DAPI	Vector Laboratories, CA (USA)

Table 5. Material used for agarose gel electrophoresis.

Agarose Gel Electrophoresis	Loading buffer (+ dye)	6x Orange DNA Loading Dye (+ SYBR Green)	Thermo Scientific, MA (USA)
	DNA ladder	O'GeneRuler™ 1kb	Fermentas, MA (USA)
	1x TAE (Tris-acetate-EDTA) buffer	40 mM Tris, 20 mM acetic acid, 1 mM EDTA	

Ticks

Ixodes ricinus adults and nymphs were used for the experiments. Nymphal ticks were collected by flagging lower vegetation in the forrest close to České Budějovice. Adult males and females were obtained from the rearing facility of the Biology Centre, Institute of Parasitology, Academy of Sciences of the Czech Republic.

Bacteria

The B31 and ZS7 strains of *Borrelia burgdorferi* (origin: J. F. Anderson, The Connecticut Agricultural Experiment Station, CT, USA) were grown at 34°C for 1 week in BSK-H medium (Sigma) with 6% rabbit serum (Sigma-Aldrich, MO, USA) and ATB [phosphomycin (0.02 mg/ml), rifampicin (0.05 mg/ml), amphotericin B (2.5 µg/ml)].

4 METHODS

4.1 *In-vitro* feeding of ticks

4.1.1 Feeding units preparation

A lens cleaning paper (Kodak ®, NY, USA) made of regenerated cellulose (rayon) is a backbone of the membrane, whose goal is to imitate the human/animal skin. The silicone mixture used for impregnation of the rayon papers causes the elasticity of the membrane and ensures closure of penetration sites to prevent a leakage of blood through the membrane. The silicone mixture consists of silicone glue RTV-1 Elastosil® E4 (Wacker, DE), silicone oil (30% DC 200; Fluka, CH), Elastosil® Color Paste FL white RAL (Wacker, DE) and hexane (Sigma-Aldrich, MO, USA). The rayon papers were attached to a sheet of glass covered with a layer of polyethylene kitchen roll, the silicone mixture was spread out on the cleaning papers and allowed to dry for about 24 hr. Afterwards, the feeding tubes were fastened to the artificial membranes using the silicone glue. The membranes of the thickness between 50 - 150 μm were used.

The membranes were checked for leaks by placing the feeding tubes into 70% ethanol for about 15 min. The leaky membranes were discarded and the feeding tubes glued to new membranes. To enhance the attachment of the ticks, a circular piece (with a radius corresponding to the radius of the feeding tube) of fiberglass mosquito netting (1.4 mm mesh) serving as a physical support was stuck onto the artificial membrane inside the feeding tube using silicone glue. Proper and uniform sticking of the mosquito netting to the membrane was ensured by applying a slight pressure on the mosquito netting. A cow hair extract was utilized as an additional tick-feeding attractant. About 70 μl of the hair extract solution were dropped to each membrane and allowed to evaporate for 30 - 60 min. A cotton-wool- in-tissue stopper was inserted into the feeding unit to confine the ticks inside.

The feeding tubes with ticks (10 females and 5 males per feeding unit) already inside were transferred into the six-well cell culture plate (Costar, USA) with pre-heated bloodmeal to 37°C in the water bath. The water bath was partially covered to increase the relative humidity in the feeding chamber and to avoid the contamination of the water in the bath.

4.1.2 Blood

Blood from rams or cattle was collected monthly from an abattoir, defribrinated with 4 mm glass beads by shaking for several minutes to form a clot attached to the glass beads. Defribrinated blood was poured into a sterilized bottle and supplemented with glucose (2 g/L) to stabilize erythrocytes and kept at 4 °C until use (Kuhnert, 1995).

To control microbial growth, gentamycin solution (5 μg/mL, Sigma, MO, USA) and nystatin solution (100 i.u./ml, Sigma) were added to the blood right before the blood was exchanged in the wells. ATP (1 mM, Fluka, CH), a tick-feeding stimulus, was added to the blood afterwards. (Values in brackets represent final concentrations in blood). All steps were done in a sterile flow-box. The 6-well plate was covered with a lid and the blood was warmed to 37 °C in the water bath before it became available to the ticks. Blood in the wells was replaced at 10 - 15 hr intervals. At each blood exchange, the lower side of the membrane, in contact with the blood, was rinsed with sterile PBS. The volume of the blood needed for one well is 3.1 mL (Kröber and Guerin, 2007c).

The *B. burgdorferi* spirochetes were added into bloodmeal at every blood exchange. 1 mL (>$3x10^7$ of bacteria) of culture medium with spirochetes was centrifuged at no more than 4 000 rpm for 5 min at RT. The supernatant was discarded and the pellet was resuspended in 1 mL of blood and transferred into the feeding chamber. In control ticks, no *Borrelia* were added to the blood.

4.2 Detection of *B. burgdorferi* within salivary glands

4.2.1 Fluorescence microscopy

For fluorescence microscopy, salivary glands and guts were dissected from partially-fed (24 and 48 post-attachment) adult ticks and placed into a 96-well microplate. The organs were immersed for 1 hr at room temperature (RT) in 4% formaldehyde/ 0.1% glutaraldehyde in 0.1 M PB solution, pH 7.4, and subsequently for 20 min at -20°C in ice cold methanol. After incubating in blocking buffer (3% BSA/ 1% nonfat-dried milk/ 0.02 M glycine in PBS[1]) for 1 hr at RT, the salivary glands and guts were incubated for 1 hr at RT (or overnight at 4°C) in rabbit polyclonal anti-*Borrelia burgdorferi* (40-50 μg/mL in PBS) and mouse monoclonal anti-OspC (20 μg/mL in PBS) antibodies. Samples were rinsed five times in ten times

[1] PBS = 0.01 M PB + 0.15 M NaCl

diluted blocking buffer. The spirochetes were detected by incubation for 60 min at RT with (FITC)-conjugated goat anti-mouse IgG (2.8 µg/mL in PBS) and/or (TRITC)-conjugated goat anti-rabbit IgG (2.8 µg/mL in PBS). Each sample was then washed five times with PBS, stained with DAPI (5 µg/mL in PBS), washed again with PBS, and mounted in polyvinylalcohol-DABCO for examination. Epifluorescence microscopy was performed on an Olympus BX-60 microscope equipped with a Olympus C-3030 ZOOM camera. Confocal microscopy was performed on an Olympus FV-1000; serial Z-series images were acquired in blue, red and green channels. In control samples, the use of primary antibody was omitted.

4.2.2 Scanning electron microscopy

For electron microscopy, isolated salivary glands from partially-fed (48 and 72 hr post-attachment) adult tick females were immersed in 2.5% glutaraldehyde in 0.1 M PB and allowed to fix at 4°C for 48 hr. They were then washed in 4% glucose in 0.1 M PB (3 x 15 min), postfixed in 2% osmium tetroxide, washed in 4% glucose in 0.1 M PB (3 x 15 min) and dehydrated by passing the specimens through a graded series of acetone-water mixtures; 30%-50%-80%-90%-95%-100% acetone. The specimens were dried in a Pelco CPD2 critical point dryer using carbon dioxide at 1200 psi, and 42°C. The dry organs were mounted on aluminium stubs using a double adhesive carbon tape. Afterwards, the samples were coated with gold using a BAL-TEC SCD-050 sputter coater, and observed and photographed by a JEOL 7401-F scanning electron microscope.

4.2.3 Correlative light electron microscopy

For correlative light electron microscopy, dissected salivary glands from partially-fed (72 hr post-attachment) adult tick females were rinsed with PBS, chemically fixed in 4% formaldehyde/ 0.1% glutaraldehyde in 0.1 M PB, pH 7.4, for 2 hr at RT, washed in 0.1 M PB with 0.02 M glycine (3 x 15 min) to block any free aldehyde groups and cryoprotected by immersion in 2.3 M sucrose for 5 days at 4°C. Sucrose infiltrated specimens were frozen by plunge freezing in liquid nitrogen, and stored in liquid nitrogen until they were sectioned. The sectioning was performed in a cryo-ultramicrotome (Leica EM UCT equipped with cryochamber Leica EM FC6). Sections of the thickness of 0.6 - 0.9 µm were obtained. Semi-thin sections were picked up using a drop of 2.3 M sucrose/ 2% methyl cellulose (1:1) (Liou *et al*., 1996) and thawed on Superfrost®Plus glass slides (Thermo Scientific, MA, USA) which were specially modified (see later in section ‘Results‘), and processed further for light

microscopy. Thawed cryosections were stored at 4°C as described by Griffith and Posthuma (Griffith and Posthuma, 2002). The sections were rinsed with distilled water at 4°C (3 x 15 min) to wash off the pick-up solution, incubated for 1 hr at RT in 5% BSA/ 1,5% nonfat-dried milk/ 0.02 M glycine in PBS. (To block non-specific binding of antibodies, 0.1% Tween-20/ 0.15 M NaCl in PBS were added in one of the experiments). Then the primary antibody (40-50 μg/mL in PBS) was applied, and the slides were incubated overnight at 4°C in a humidified chamber. After six times washing with 0.05% Tween-20 in PBS, the specimens were labeled with the secondary antibody (2.8 μg/mL in PBS) at RT. Sections were washed six times with 0.05% Tween-20 in PBS and mounted with Vectashield (with DAPI) antifade and coverslipped. Images were acquired by epifluorescence (Olympus BX-60) and confocal microscopy (Olympus FV-1000).

After examination with fluorescent microscopy, the specimens were processed further for scanning electron microscopy. The sections were incubated overnight at 4°C in PBS to soften the mounting medium, the cover slip was removed and the specimens washed five times with PBS. The slides were incubated for 30 min at RT in 5% BSA/ 1.5% nonfat-dried milk/ 0.02 M glycine in PBS. Then the sections were loaded with the mouse anti-FITC (1:40 in 1x diluted blocking buffer) tertiary antibody conjugates to 10 nm gold particles (Aurion, NL) for 90 min at RT, followed by washing (thrice in PBS or 0.05% Tween-20 in PB containing 0.3 M NaCl). To stabilize the ultrastructure and enhance the contrast for SEM, the specimens were post-fixed in 1% osmium tetroxide for 1 hr at RT. The slides were then washed twice with PBS. To minimize tissue distortion, the specimens were dehydrated in a graded ethanol series from water through 30%-50%-80%-90%-95%-100% ethanol, followed by dehydration in ethanol:t-butyl alcohol (2:1; 1:1; 1:2) mixture. Every step took about 3 min at RT. Afterwards, the glass slides were incubated in 100% tertiary butanol for about 15 min at 4°C. The samples were freeze-dried under vacuum in a BAL-TEC SCD-050 sputter coater. The frozen t-butyl alcohol was completely sublimated after 30 min. The glass slides were broken apart and the pieces with specimens were fastened on an aluminium specimen carrier using a double stick tape. The samples were coated with gold in a BAL-TEC SCD-050 sputter coater for 20 sec right before the microscopy examination. Scanning electron microscopy was performed by a JEOL 7401-F. Schematic outline of the correlative light electron microscopy procedure is depicted in the Figure 3 below.

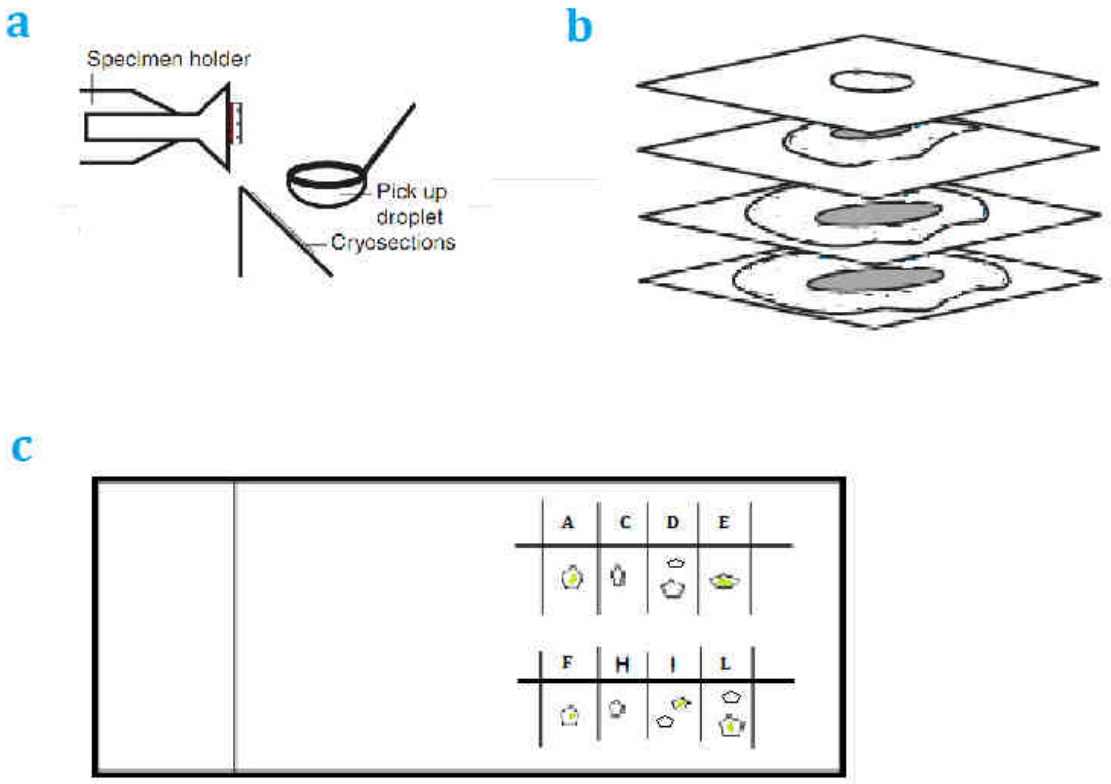

Figure 3. Schematic overview of CLEM procedure. (**a**) The specimen infiltrated in sucrose is sectioned with a diamond knife. Cryosections are collected with a drop of methylcellulose/sucrose solution and transferred to a glass side. (**b**) A z-dimension stack of cryosections cut on the ultramicrotome. (**c**) A gridded glass slide with a simplified mapping system enabling easy localization of the fluorescing sections (here A, E, F, I, L) in the electron microscope.

Comment:

A high-scale sample preparation for fluorescence microscopy is a very tedious process. To set up a 96-well plate, it takes thousands of pipetting steps. In addition, when working with very small samples, much of the material gets lost during the whole laborious procedure. To speed it up and to make sure that no specimens are wasted, we were advised by Yannick Schwab (IGBMC, Strasbourg) to use the following methodology:

The 1 mL pipette tips are cut about 2 cm from narrow ending. The narrow end is heated up to melt slightly and glued to fine net fabric (Figure 4b). The sample is placed inside the cut tip onto the fabric. Several such modified tips are inserted into each other. Using the pipett the samples are flushed with desired solution (Figure 4a). Make sure that the cut pipette tips fit correctly. Otherwise it is not possible to pull up the liquid.

This methodology worked well but it did not completely solve our problem of high-scale sample preparation. We did not have so many pipettes available. Futhermore, the samples may be mutually contaminated. Therefore, we modified the system to fulfil our needs. Again, the sample was placed inside the cut tip. But this time, the 96-well plate was pre-filled with the desired solutions (fixation, blocking and washing buffers, antibodies, etc) and transferred the tips from well to another (Figure 4c). This allowed us to skip all the tedious "pipette-in" and "pipette-out" steps, which one has to endure under normal circumstances. This technique saves a lot of time, samples and nerve cells.

Figure 4. Cut pipette tips glued to fine net fabric and **(a)** attached to the pipette; **(b)** in detail; **(c)** placed in the 96-well plate.

4.3 Detection of plamids

B. burgdorferi were grown to a density $>10^7$/mL in BSK-H culture medium.

4.3.1 DNA extraction

For DNA extraction a Wizard® Genomic DNA Purification Kit (Promega) was used. The original procedure for 'Isolating Genomic DNA from Gram Positive and Gram Negative Bacteria' was slightly modified. *Borrelia burgdorferi* culture (8-10 mL; $>10^7$ spirochetes/mL) was centrifuged at 8,000 rpm for 10 min at 20°C to pellet the cells. The supernatant was removed and 600 µL of Nuclei Lysis Solution were pipetted to the cells. After 5 min at 80°C, the lysate was cooled down to RT and 3 µL of RNase Solution was added, then allowed to incubate for 15 min at 37°C. Afterwards, 200 µL of Protein Precipitation Solution was added and allowed to incubate for 5 min on ice. The sample was centrifuged at 13,000 rpm, the supernatant containing the DNA was transferred to a 1.5 mL microcentrifuge tube containing 600 µL of isopropanol and gently mixed by inversion. The

sample was centrifuged again at 13,000 rpm for 10 min at 10°C. The supernatant was poured off and 600 µL of 70% ethanol were added to wash the pellet. Afterwards, the sample was centrifuged at 13,000 rpm for 10 min at 10°C. Ethanol was drained carefully and the pellet was allowed to air-dry for 10 min. Finally, 100 µL of DNA Rehydration Solution were added and the DNA was stored overnight at 4°C to fully rehydrate.

4.3.2 PCR Analysis

The presence of individual plasmids was confirmed by PCR. Preparation of PCR mixture (per reaction) is summarized in Table 6. The program used for amplification is presented in Table 7. The primers used in the PCR reaction are presented in Table 8.

Table 6. Components for a single reaction mixture for PCR amplification.

component	volume (µL)
10x PCR Reaction Buffer (Qiagen)	2
dNTPs mix (contains 1.25 mM/each dNTP)	2
Primers (F + R) (20 pmols)	1 + 1
HotStarTaq DNA Polymerase (Qiagen)	0.1
dd H_2O	12.9
DNA Extract (approx. 50 ng)	1
total	**20**

The PCR reaction mixtures were pipetted into a 96 well PCR plate. PCR was run on a Bio-Rad T100™ Thermal Cycler under the following conditions:

Table 7. Program for PCR.

step		temperature (°C)	time
1	initialization	94	5 min
2	denaturation	94	30 sec
3	annealing	55	30 sec
4	elongation	72	1 min
5	Cycle to step 2 for 29 more times		
6	final elongation	72	7 min

Table 8. Primer sets specific for plasmids of both *B. burgdorferi* B31 and ZS7. Lp25(a) and lp25(g) designate oligonucleotides specific for *B. afzelii* and *B. garinii*, respectively.

Plasmid	Primer	Sequence
cp9	F4568	5' GGA CTG GTA TTT ACT CCG GCT GAT AGA GC 3'
	R4569	5' CCT TAA TGA TGA GGC CGA TGA AGT TGC 3'
lp17	F4507	5' ACT GCA ATC TGC CCA AGC TAC ATA ATC T 3'
	R4508	5' AAG GTA AGG ACG GTT GTC TAC ATG GAT T 3'
lp21	F4562	5' TGT GGT TGC TAA AAC CCA AGC GT 3'
	R4563	5' TTG TTT CTA ATT GCT CTG AAT TGC ATC C 3'
lp25	F4511	5' AGA ATT ATG TCG GTG GCG TTG T 3'
	R4484	5' ATT AAA GCC GCC TTT TCC TTG GT 3'
lp25(1)	F4596	5' TTG CTG CCA TTT CTC ACT TGG TAA 3'
	R4597	5' ATA AAA GCG ACA GGT TAT CGT GCA G 3'
lp25(2)	-	5' GTG CAC CTA TTG GAA AGG TC 3'
	-	5' GGG CAT GTT GCA CAT ACG TT 3'
lp28-1	F4340	5' CGG GGA TCC AGC CAA GTT GCT GAT AAG GAC GAC CC 3'
	R4084	5' ACG GCA GTT CCA ACA GAA CCT GTA CTA TCT 3'
lp28-1(1)	F4598	5' TTC TGA TGG CAC TGA GCA AAC CA 3'
	R4599	5' AAC CCT TTA CAC TTT CTT CGA TTG CGC T 3'
lp28-2	F4523	5' CCC TCA TCA AGT TTT TCC ATG TGT TTT T 3'
	R4524	5' AGG TGG CCT TTC CGA GCT TGT ACC TTA C 3'
lp28-3	F4534	5' AAC ACT ATC TTA AAT GTC CCC CAC AA 3'
	R4535	5' GTG GAA GAG TGG TTA TGG TCA ATT TT 3'
lp28-4	F4525	5' TCA CCT CAG CTA ATC TAT TTA TCG ACA C 3'
	R4526	5' AAG CGC GGA GTT TTC GGC TG 3'
lp36	F4518	5' TTC TTA TCC CTG ACT TTC ACT TTT GAG G 3'
	R4519	5' TCC TTT ACT TCT ATG TTT TTA CTT TCC TTG GT 3'
lp38	F4505	5' AGC A/GGC AGA ACA AAA CAT GCA AAA ACT G 3'
	R4506	5' TCC AAG CTA TTT CTA CGG CCT CTT TAG C 3'
lp54	F4538	5' GCA AAA TGT TAG CAG CCT TGA CGA GAA A 3'
	R4539	5' TAG ATC GTA CTT GCC GTC TTT GTT TTT T 3'
lp56	F4566	5' ACT ATT AAG ACG AGC AAT AAA AAG TCC A 3'
	R4567	5' GAC GAA GCA AAG AAG GAT TTG GAT CAC C 3'
cp26	F4536	5' ATA GCC CAT TCC AGA CAT TAA ACC GCC T 3'
	R4537	5' AGT TCC CCA AAT AAC AGC AAT CTG CGA 3'
cp32-1	F4571	5' ACG ATA GGG TAA TAT CAA AAA AGG 3'
	R4572	5' AGT TCA TCT AAT AAA AAT CCC GTG 3'
cp32-2	F4577	5' GGA ATG TAT TAA TTG ATA ATT CAG 3'
	R4578	5' GCG AAC TAA ATA GTG CCT TAT GGG 3'
cp32-3	F4529	5' GCA AGT TCC CAC GAT AAC ACA CCC GTA T 3'
	R4530	5' TTT TCA TAT CCC CTC CTA GCT TTA TTG CC 3'
cp32-6	F4575	5' GAC TTT ACA TAG TAT AAA TGC TTT TGG 3'
	R4576	5' TCT CGT TAT TAT AAA ATA AGT AGG 3
cp32-8	F4579	5' GAA GAT TTA AAC AAA AAA ATT GCG 3'
	R4580	5' GTA ATC ACT TCT TTT TTA CCA TCG 3'
cp32-9	F4581	5' TAT CAA AAA AGT GCT GTT TTA TAG 3'
	R4582	5' TAA TCT CAA ATA TTC TTC TTT ATG 3'
lp25(a)	-	5' ACG CAG ATG GGG TGG GGG AT 3'
	-	5' GGC AGT GGC GGT CCT TCT GC 3'
lp25(g)	-	5' TGT GCC GGC TTT GTC GTC GG 3'
	-	5' GTG CCC ACA CTC TAT TGC ACG GG 3'

4.3.3 Agarose gel electrophoresis

Agarose Gel Electrophoresis was run according to the 'Liberty 120 High-Speed Gel System (Biokeystone, USA)' user manual. Supplementary information:

- 1% agarose (in 1x TAE buffer) gel was used
- 1x TAE was used as running buffer
- gel run at 250 V, 25 min

4.4 Microscopy examination of *I. ricinus* nymphs molting to adults

4.4.1 Light microscopy observation of internal morphology

Four molting nymphs (2 in early-molting phase and 2 in advanced-molting phase) were dissected to confirm/disprove the presence of the salivary gland acini. During the investigation, images of the ticks inner structure were acquired to give insights into the morphological changes that accompany the nymph metamorphosis. The examination was performed by a Olympus SZX-10 stereomicroscope.

4.4.2 Fluorescence miscroscopy examination of salivary glands

The salivary glands isolated from nymphs in the advanced-molting phase were immersed for 1 hr at RT in 4% formaldehyde/ 0.1% glutaraldehyde in 0.1 M PB solution, pH 7.4, and subsequently for 20 min at -20°C in ice cold methanol. After incubating in blocking buffer (3% BSA/ 1% nonfat-dried milk/ 0.02 M glycine in PBS) for 1 hr at RT, the organs were stained in rabbit polyclonal anti-Borrelia burgdorferi (40-50 μg/mL in PBS), washed six times with 0.05% Tween-20 in PBS, incubated for 1 hr at RT in (TRITC)-conjugated goat anti-rabbit IgG (2.8 μg/mL in PBS), washed six times with 0.05% Tween-20 in PBS and stained with DAPI (5 μg/mL in PBS). The specimens were washed four times with 0.05% Tween-20 in PBS and mounted with PVA-DABCO antifade and coverslipped. The images were acquired by a confocal microscope Olympus FV-1000.

5 RESULTS

5.1 *In-vitro* feeding

Ticks *Ixodes ricinus* were used for the *in-vitro* feeding (Figure 5). The attachment rate of adult ticks fluctuated around 70%. The ticks were not pretreated in any way before the onset of the feeding. Artificial silicone membranes of thickness between 60 - 150 µm were employed successfully. Addition of a plastic gasket with a radius that precisely fits into the glass feeding tube prevented the ticks from getting stuck to the membrane, therefore, it considerably reduced the tick mortality rate.

After successful implementation of *in-vitro* feeding system for adult ticks, we attempted to adjust the set for nymphal feeding. The membrane of thickness around 55 µm was used and additional components such as a plastic cross (Figure 5a) were utilized. Unfortunately, the nymphal feeding has not been brought to successfull end yet. Almost all the nymphs died during the procedure.

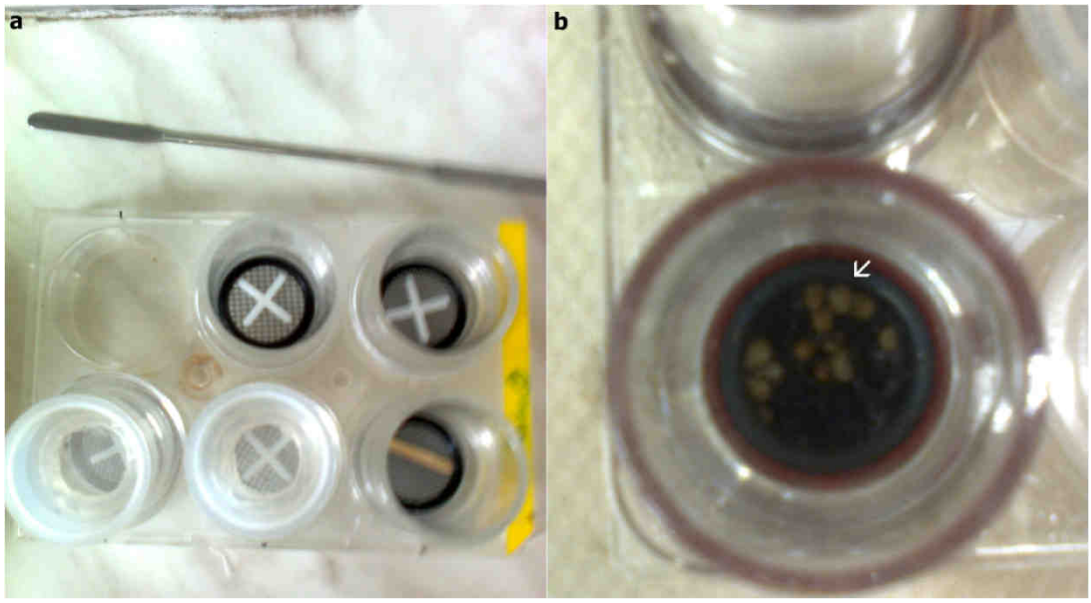

Figure 5. **(a)** Six-well plate with feeding units. A plastic cross to provide additional border. **(b)** One feeding unit depicting the *I. ricinus* ticks feeding on blood through the membrane. A gasket (arrow) to prevent ticks from attachment to the silicone-excessive part of the membrane.

5.2 Detection of *Borrelia* using immunofluorescence microscopy

At the 24-hour time point (one day after attachment), high numbers of each low-passage *B. burgdorferi* ZS7 and high-passage *B. burgdorferi* B31 were observed in the gut of ticks, yet not in the salivary glands. The spirochetes in the gut were mostly OspC-negative, only few specimens close to the gut surface expressed this lipoprotein (Figure 6b). At the 48-hour time point, the low-passage strain was already present within the salivary glands, namely on the acinar surface and in/on the salivary ducts (Figure 6f-h). The numbers of spirochetes varied, we estimate 20 organisms per salivary gland. The high-passage strain also appeared in the salivary ducts, however, very sporadically (i.e. <5 spirochetes/salivary gland), and in only very few samples (Figure 6e).

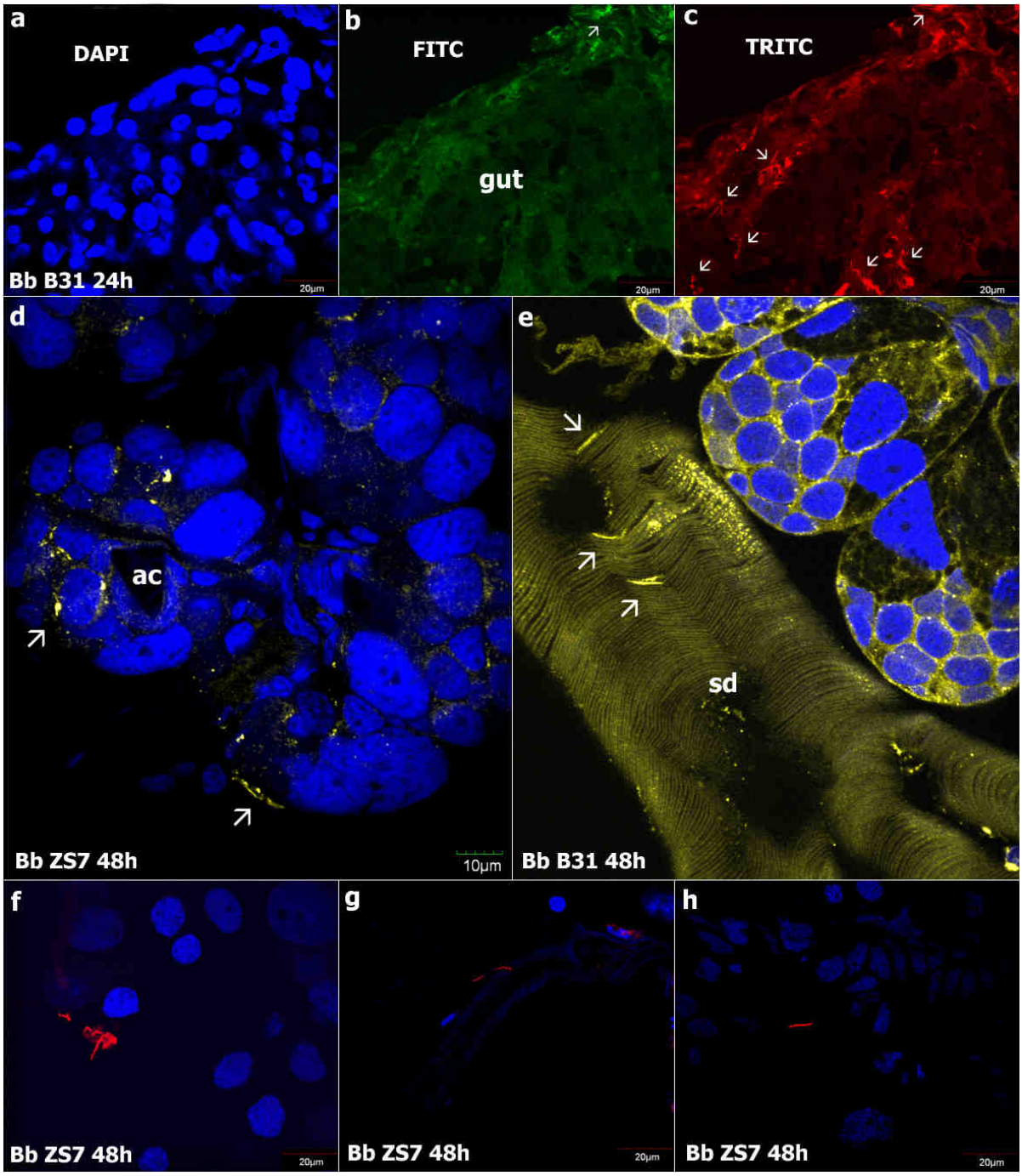

Figure 6. Localization of *B. burgdorferi* spirochetes within the tick gut and salivary glands by a Olympus FV-1000 confocal microscope. **(a - c)** Presence of *B. burgdorferi* B31 (arrows) in the gut tissue at 24 hr; **(a)** DAPI counterstaining, **(b)** detection of OspC-positive spirochetes, **(c)** detection of spirochetes with rabbit anti-*B. burgdorferi* and TRITC-labeled anti-rabbit antibody. **(d-h)** Presence of *B. burgdorferi* ZS7 (passage 3-4) and B31 (passage 15) within the salivary glands; merged images, nuclei stained with DAPI, spirochetes with rabbit anti-*B. burgdorferi* and TRITC-labeled anti-rabbit antibody. **(d, f, h)** Spirochetes on the surface of granular acini (ac), **(e, g)** *Borrelia* associated with the salivary duct (sd); '**d**' and '**e**' images, the color of TRITC was changed to yellow for better visibility of spirochetes.

5.3 Detection of *Borrelia* using scanning electron microscopy

Once *B. burgdorferi* ZS7 were positively localized in the tick salivary glands by using immunofluorescence confocal microscopy, we attempted to obtain detailed structural information of the tissue-spirochete interaction by using scanning electron microscopy. At 48 and 72 hours after attachment, the salivary glands were isolated, fixed, dehydrated, dried, and coated with gold. No antibody labeling of the spirochetes was performed. Unfortunately, this methodology did not allow us to observe any spirochetes within the salivary glands. As it turned out, the amount of bacteria in the tissue was too low, furthermore, the surface of the salivary glands was covered occasionally with fibre-like contaminations, which made the unambiguous spirochete identification impossible (Figure 7).

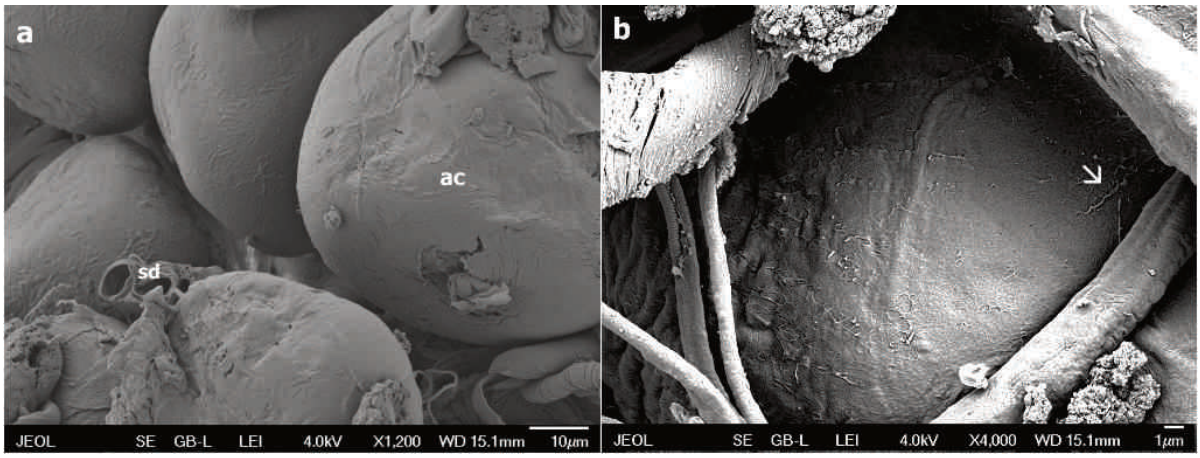

Figure 7. Scanning electron microscopy of salivary glands isolated from females *Ixodes ricinus* infected with *B. burgdorferi* B31 at 72 hr after attachment. (**a**) Low magnification overview showing a part of the salivary acini (ac) and salivary duct (sd). (**b**) Potential spirochete on the acinar surface (arrow).

5.4 Pilot trials of detection of *Borrelia* using correlative light electron microscopy

To overcome the difficulty with the bacteria localization on electron microscopes, we decided to employ a recently emerging technique - correlative light electron microscopy. At 72 hours after attachment, the salivary glands were isolated, cut to sections and prepared for

immunofluorescence microscopy to reveal the presence of *Borrelia*. Afterwards, the same specimens were modified so that they can be viewed by using scanning electron microscopy.

Before the desired *Borrelia* localization within the salivary glands could be accomplished, we had to overcome many obstacles throughout the exacting procedure.

- First, a widget that enable easy processing of sample sections has been invented. We have developed a mapping system that noticeably accelerated the retrospective localization of the region of interest (sample sections with *B. burgdorferi* spirochetes in our case) (Figure 8).

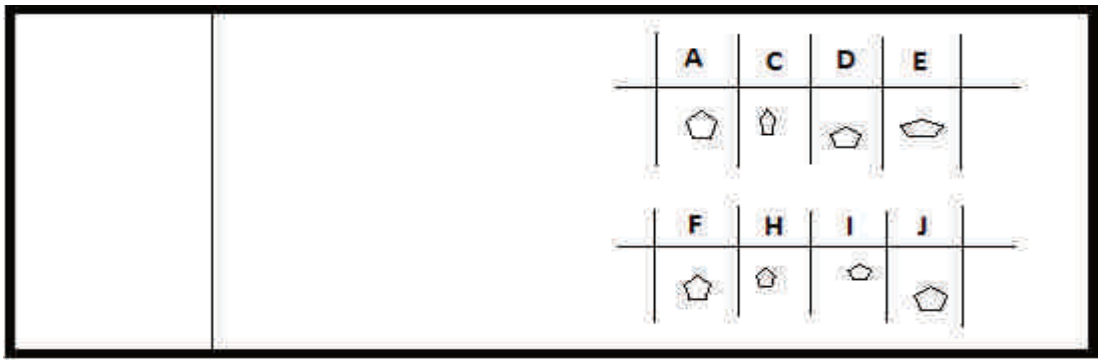

Figure 8. A simplified system of coordinates was curved into the glass slide by using a diamond knife. When a positive (fluorescing) section was spotted, the appropriate letter was written down. Afterwards, when the glass slide was examined on the electron microscope, the location of the region of interest was determined with ease.

- Secondly, the procedure of specimen preparation is immensely difficult. The sample had to be manipulated in a way that it is possible to examine it both on light and electron microscopes, though each device works under considerably different operating conditions. The procedure that is listed in a section ‘Methods‘ is the one with which the best results were obtained; lowest autofluorescence and non-specific antibody binding together with best structural preservation.

- Thirdly, the operating parameters of the scanning electron microscope were optimized.

1. **Detector -** Three different detectors were tested to determine, which gives the best images; two secondary electron detectors: an upper detector (**SEI**) and a lower detector (**LEI**), and an Autrata **YAG** (yttrium aluminium garnet) backscattered electron detector. The SEI mode gave better resolved images, however, because of the surface charging it was not suitable for the analysis. The better results were achieved by LEI and YAG detectors. The LEI mode provided good topological contrast with very low charging. The YAG detector was of choice when the gold nanoparticles were detected, since here an output signal that is generated is based upon the difference in the atomic number, therefore, giving the best contrast enabling the localization of nanoparticle markers.

2. **Working distance (WD) -** WD is the distance between the front edge of the objective lens and the specimen surface. We determined that 12 - 15 mm is an optimum distance which provided the best image quality when LEI and YAG detectors were used.

3. **Accelerating voltage -** The best image quality was obtained with accelerating voltage between 4-6 kV. The output signal was degraded with voltage lower than 3 kV, giving inferior contrast. On the other hand, higher voltage caused charging of the sample and its deterioration.

Despite enormous effort (the procedure was repeated at least ten times with various staining protocols), the successful localization of *Borrelia* using correlative light electron miscroscopy has not yet been accomplished. The biggest difficulty encountered so far is the chitin autofluorescence of the salivary ducts and the non-specific antibody binding. When the samples were sectioned, it readily happened that the salivary ducts cross-sections strongly fluoresced, and therefore resembled (even in shape) the spirochetes.

See the images (Figure 9 and 10) acquired by fluorescence and scanning electron microscopes.

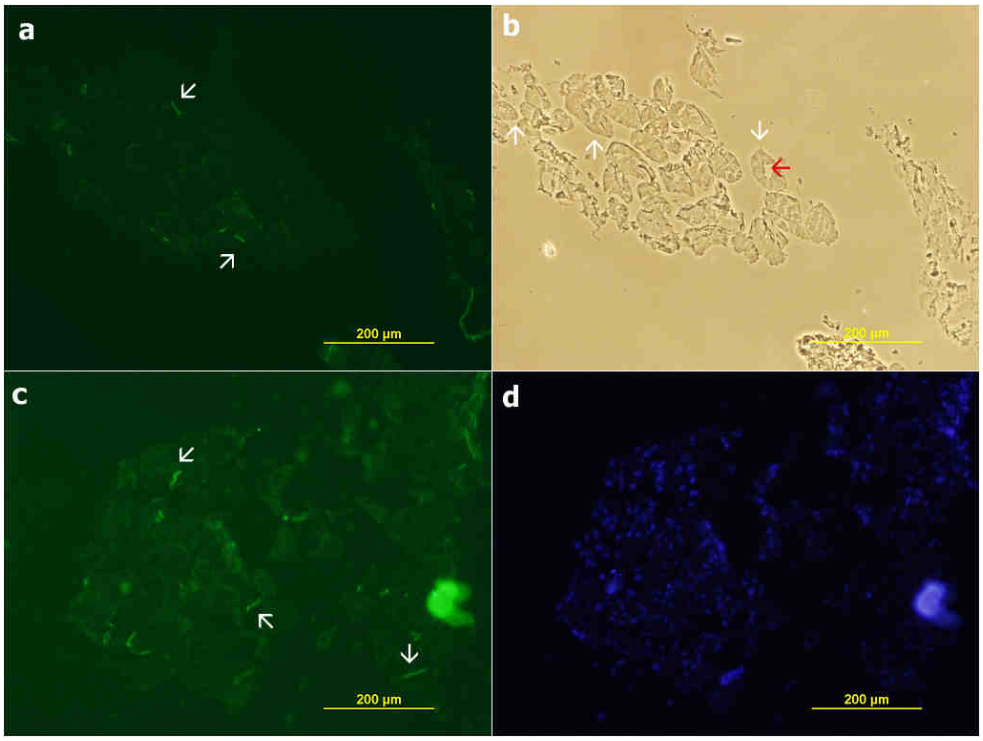

Figure 9. Localization *B. burgdorferi* ZS7 (passage 4) within salivary glands on thawed cryosections by using correlative ligh electron microscopy. (**a**) Detection of spirochetes with rabbit anti-*B. burgdorferi* and FITC-labeled anti-rabbit antibody. Here, however, the spirochete-like objects (arrows) are not *Borrelia*, but false positives caused by non-specific antibody binding as revealed by using SEM. (**b**) The same section taken with Nomarski objective showing the salivary gland acini (arrows). (**c**) Again, as in the picture '**a**', non-specific antibody binding and chitin autofluorescence of the salivary ducts hindered the localization of *Borrelia* spirochetes. (**d**) DAPI staining.

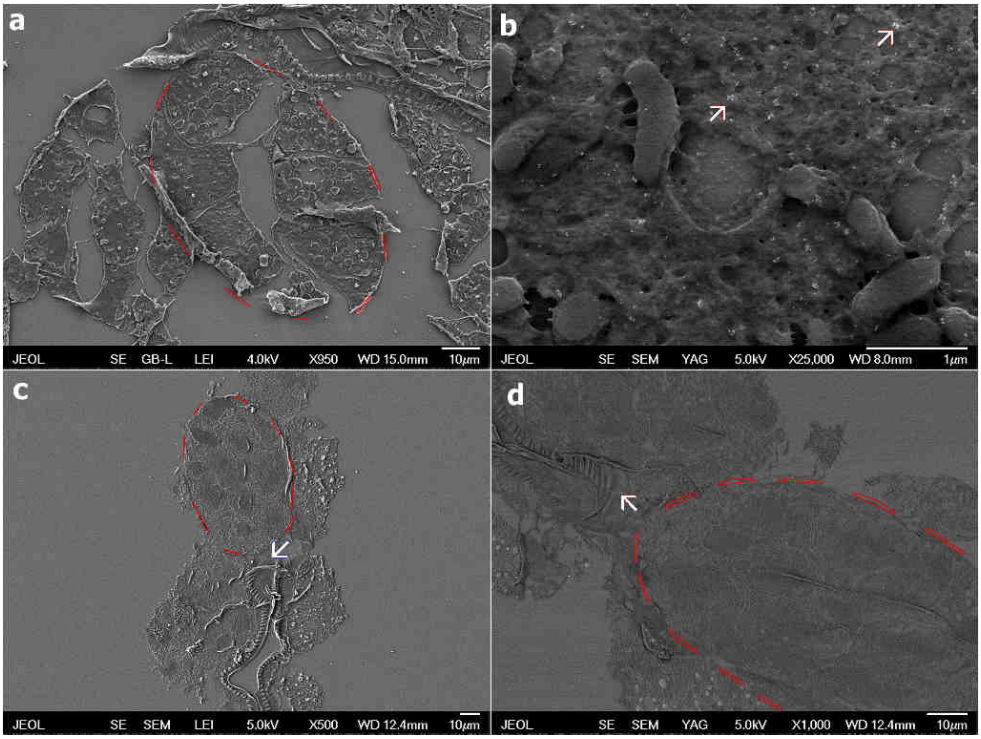

Figure 10. Salivary glands on cryosections imaged by using scanning electron microscopy. (**a**) Salivary gland acinus (highlighted) with fine structural details, but partial material loss. (**b**) Surface of the salivary gland acinus with non-specifically bound gold nanoparticles (arrows). (**c**) Salivary gland acinus (highlighted) with very good structural preservation and a salivary duct draining into the acinus (arrow). (**d**) Again, salivary gland acinus (highlighted) with ideal structural preservation and a salivary duct draining into the acinus (arrow).

5.5 Correlation of plasmids and dissemination ability

To clarify the above findings concerning the different dissemination propensity of low- and high-passage *Borrelia*, we checked and compared the plasmid profiles of these *Borrelia*. It has been shown by others (Purser and Norris, 2000; Labandeira-Rey and Skare, 2001), plasmids are the decisive factors of borrelial infectivity. The bacterial DNA was extracted, plasmid primers were used and completed PCR reactions were loaded onto the agarose gel for electrophoretic separation. In the first run, low-passage (6) *B. burgdorferi* ZS7 (Figure 11) and high-passage (>15) *B. burgdorferi* B31 (Figure 12 and 13) were examined. Low-passage (5) *B. burgdorferi* B31 were used as positive control (Figure 14).

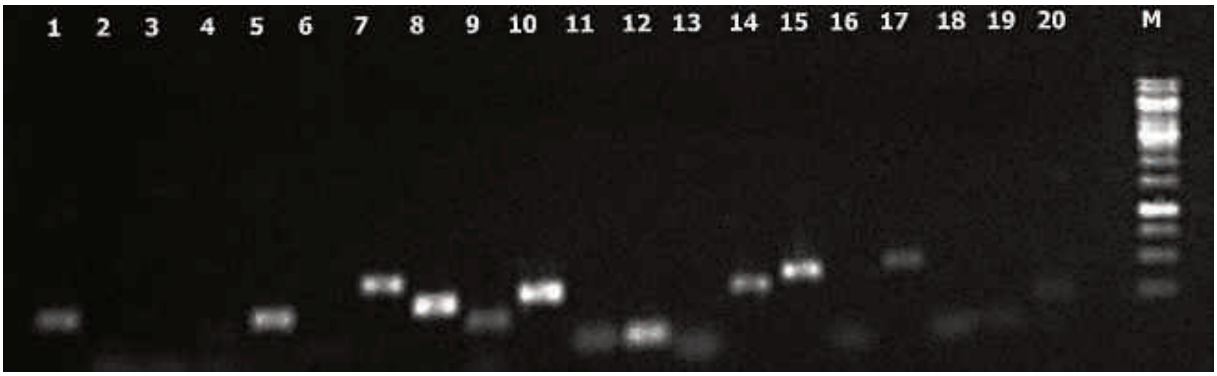

Figure 11. Plasmid profile of *B. burgdorferi* ZS7 (passage 6). Lp17, lp28-1, lp28-2, lp28-3, lp28-4, lp36, lp54, cp26, cp32-1, cp32-3 are present. Column numbers are assigned to particular plasmids in Table 9 below. M - O'GeneRuler™ 1kb DNA ladder.

Table 9. Column number with a respective plasmid.

Column	1	2	3	4	5	6	7	8	9	10
Plasmid	lp17	lp21	lp25	lp25(1)	lp28-1	lp28-1(1)	lp28-2	lp28-3	lp28-4	lp36
Column	11	12	13	14	15	16	17	18	19	20
Plasmid	lp38	lp54	lp56	cp26	cp32-1	cp32-2	cp32-3	cp32-6	cp32-8	cp32-9

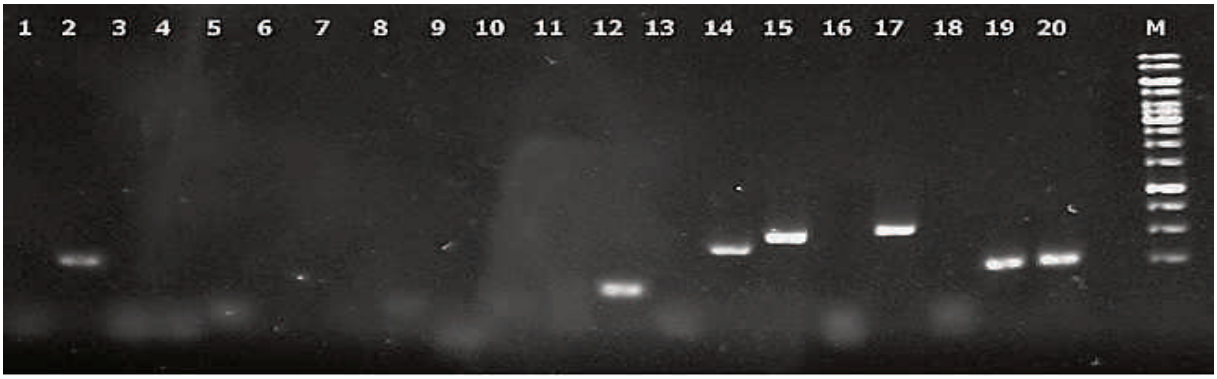

Figure 12. Plasmid profile of *B. burgdorferi* B31 (passage 17+). Vast majority of plasmids was lost during *in-vitro* cultivation. Only 7 plasmids remain (lp17, lp54, cp26, cp32-1, cp32-3, cp32-8, cp32-9). Column numbers are assigned to particular plasmids in Table 10. M - O'GeneRuler™ 1kb DNA ladder.

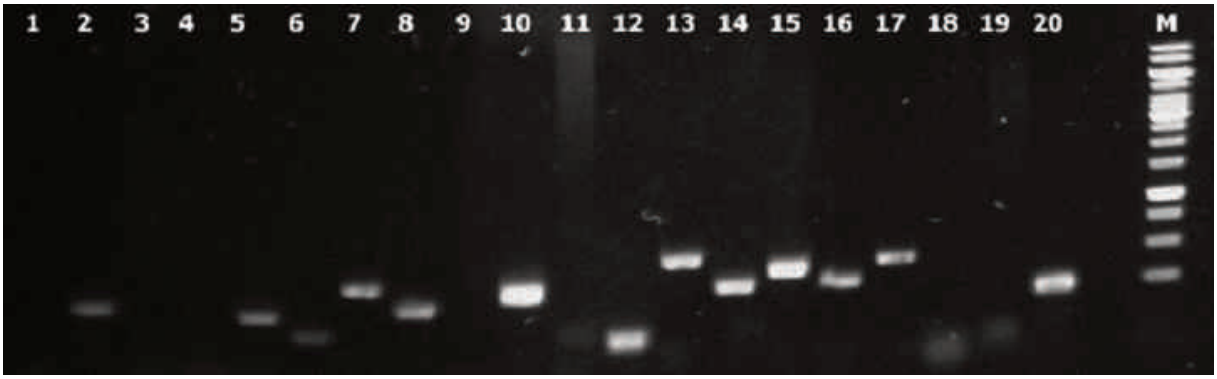

Figure 13. Plasmid profile of *B. burgdorferi* B31 (passage 21). Several plasmids are missing (cp9, lp21, lp25(1), lp28-4, lp38, cp32-6, cp32-8. Column numbers are assigned to particular plasmids in Table 10. M - O'GeneRuler™ 1kb DNA ladder.

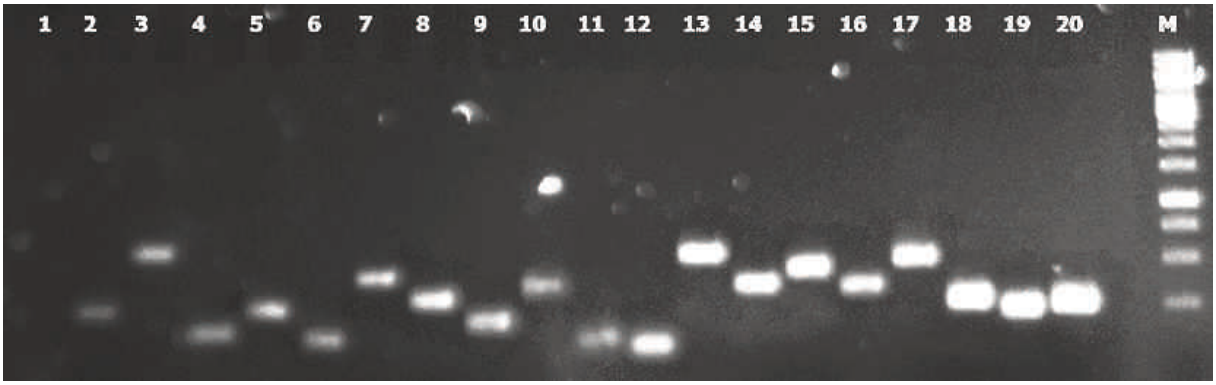

Figure 14. Plasmid profile of the control sample; *B. burgdorferi* B31 (passage 5). All but one plamid (cp9) are present. Column numbers are assigned to particular plasmids in Table 10 below. M - O'GeneRuler™ 1kb DNA ladder.

Table 10. Column number with a respective plasmid.

Column	1	2	3	4	5	6	7	8	9	10
Plasmid	cp9	lp17	lp21	lp25(1)	lp28-1	lp28-1(1)	lp28-2	lp28-3	lp28-4	lp36
Column	11	12	13	14	15	16	17	18	19	20
Plasmid	lp38	lp54	lp56	cp26	cp32-1	cp32-2	cp32-3	cp32-6	cp32-8	cp32-9

From the obtained plasmid profiles it is apparent that our *B. burgdorferi* B31 (passage 17+) isolate contained much less plasmids than the isolate designated as *B. burgdorferi* B31 (passage 21), indicating that the number of passages in this instance did not correspond to the reality, or that it is a different *Borrelia* strain. Nevertheless, we focused on the plasmids that were proven to be connected with pathogenesis and infectivity in the mammalian host and in the ticks. Namely, lp25, lp28-1, lp36, lp54, and cp26. Lp54 and cp26 were present in all tested isolates. *B. burgdorferi* B31 (passage 17+) lacked lp25, lp28-1, lp36, meaning that

this isolate should be able to disseminate within tick a vector, but it should not be infective for a host. *B. burgdorferi* B31 (passage 21) and *B. burgdorferi* ZS7 (passage 6) possessed all of the aforementioned essential plasmids but lp25.

New PCR analysis was performed to make sure that lp25 is really absent. This time with three different sets of primers against lp25 of *B. burgdorferi* and one set of primers against lp25 of *B. afzelii* and *B. garinii*. The control detection corrected the previous results. *B. burgdorferi* B31 isolates still lacked lp25, however, it turned out *B. burgdorferi* ZS7 possessed this linear plasmid (Figure 15).

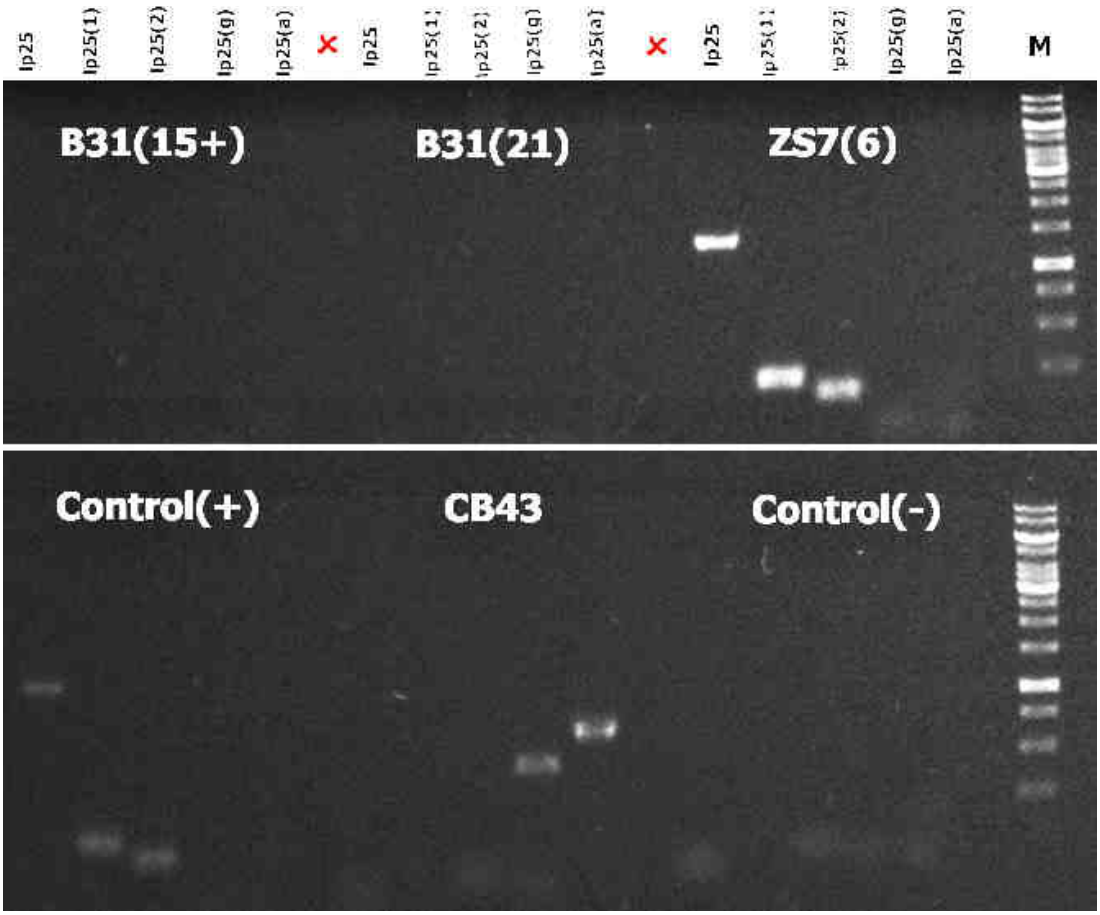

Figure 15. Control detection of the lp25 within the different borrelia isolates. It showed up that *B. burgdorferi* B31 (passage 15+ and 21) really lacked this plasmid in the genome. *B. burgdorferi* ZS7, however, contained the lp25. The lp25 of the CB43 strain of *B. afzelii* was detected by primers denoted as **lp25(g)** and **lp25(a)**. These are primers designed for screening *B. garinii* and *B. afzelii*, respectively. **Lp25**, **lp25(1)** and **lp25(2)** denote three different PCR primer sets specific against lp25 of *B. burgdorferi* B31 and ZS7. Negative control: PCR run without DNA. Positive control: DNA of *B. burgdorferi* B31 (passage 5).

5.6 Light microscopy examination of nymphs molting to adults

Two infected nymphs in the early-molting phase and two in the advanced-molting phase were examined to confirm the presence of the different salivary gland acinar cells during metamorphosis, i.e. to probe the possibility of transstadial transmission of *Borrelia* within the salivary glands. The salivary glands were observed within all four ticks by light microscopy. Unfortunately, the salivary glands from the nymphs in the early-molting phase (new cuticle is not present yet) were too minuscule, so it was not possible to pick them up and examine more thoroughly, i.e. to determine, which types of acini (I, II and III) were present. The salivary glands from the nymphs in the later-molting phase (new cuticle is already present) were isolated successfully and examined. Fluorescence microscopy confirmed that type-II and -III acini were present (Figure 16). Optical microscopy affirmed the presence of type-I acini (Figure 18 in Appendix). The antibody specific for *Borrelia burgdorferi* did not convincingly prove the occurence of the spirochetes (Figure 19 in Appendix).

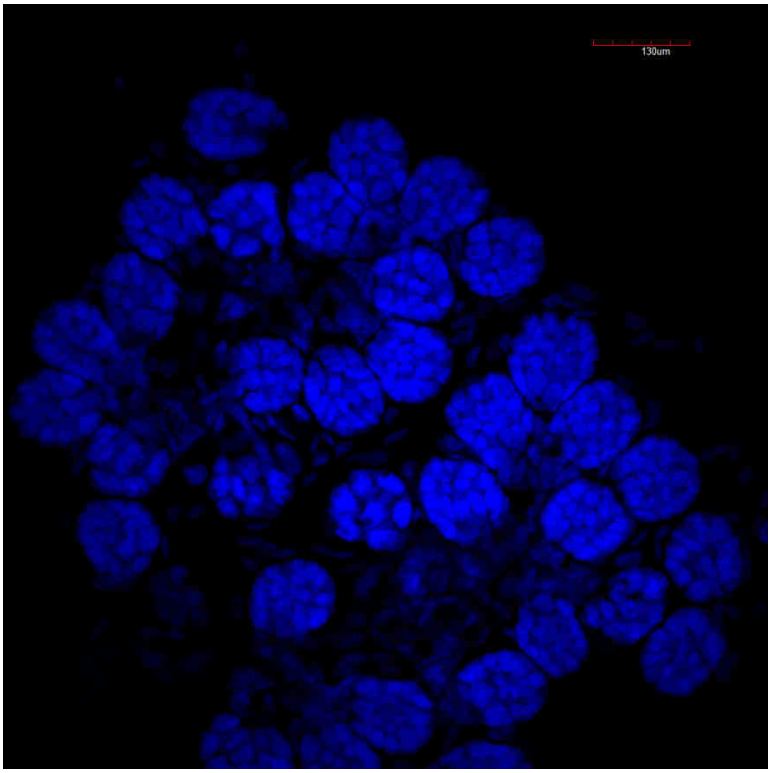

Figure 16. Salivary glands of molting *Ixodes ricinus* nymphs. DAPI nuclear counterstain confirmed the presence of the granular (type-II and -III) acini.

6 DISCUSSION

6.1 *In-vitro* feeding

The procedure described in the section 'Methods' is a slightly modified version of the original created and described by Kröber and Guerin (2007b). This method has been so far, to the best of our knowledge, successfully applied to only adult *Ixodes ricinus* ticks. The attachment efficacy is strongly dependent on ticks used in the experiment, strictly speaking, on the size of their hypostome (Tajeri and Razmi, 2011).

Kröber and Guerin (2007c) achieved an attachment rate of no less than 75% with ticks *I. ricinus*. Our attachment rate fluctuated around 70% with the same species. However, we omitted some of the prolonged preconditioning steps. For instance, they reported that ticks must be pretreated for 3 weeks at 20 to 23°C and 85% to 98% relative humidity to enhance attachment. We completely left out this phase and used ticks that underwent no special pretreatment. The reason behind this decision was, besides saving time, that in our first trials the preconditioning had rather negative influence on the well-being of the ticks. Furthermore, cow hair cut serving as an additional feeding stimulant in experiments carried out by Kröber and Guerin (2007b) was not applied during our experiments. They also stated that the thickness of the artificial membrane should not exceed 110 µm. We successfully utilized membranes of thickness between 140 - 150 µm, with no apparent impact on attachment rate. The problem that we had to face during our trials was that ticks preferentially attach at the margin of the membrane, where the glass feeding tube is glued to the artificial membrane. That means, at a place where redundant silicone glue frequently covers the surface of the membrane, making it very sticky and impenetrable for the tick hypostome. We addressed this challenge by using a plastic gasket with a radius that precisely fits into the glass feeding tube. It prevented the ticks from getting stuck to the membrane, therefore, it considerably reduced the tick mortality rate. In the latest experiments, we have even omitted the use of a cow hair extract. No adverse effects of this step have been observed so far. Last but not least, Kröber and Guerin worked with a thermostatted water bath with a tilted cover to keep the air above the feeding chambers near 100% relative humidity. In our experience, the increased humidity negatively influenced fitness of the ticks, making them more susceptible to death.

The silicone-mebrane based *in-vitro* feeding system has proven itself as a powerful technique to obtain infected adult ticks. Addition of a plastic gasket has turned out to be an astute manoeuvre, which prevents ticks from attachment to the silicone-excessive part of the membrane. The reason why, in our case, the increased relative humidity adversely influenced fitness of adult ticks during feeding might reside in that we did not precondition the ticks in any way, therefore, they were not competent to sustain such an intense environmental change. The average attachment rate oscillated around 70%. It is a value comparable with conventional feeding on animals, and therefore, fully satisfying. Speaking in general, *in-vitro* feeding has an unquestionable advantage over *in-vivo* feeding in that no ethical issues must be considered. It saves lifes of animals, not to mention the money spent on their rearing.

After successful implementation of *in-vitro* feeding system for adult ticks, we attempted to adjust the set for nymphal feeding. Size of hypostome of *I. ricinus* nymphs is about 170 µm (Kröber and Guerin, 2007a). Therefore, the thickness of the artificial membrane with which we have mostly worked so far (90 - 130 µm) should have been thin enough to allow the nymphs penetrate the barrier. However, it showed up that it was an incorrect presumption. Afterwards, the thickness of the membrane was decreased down to about 55 µm. However, the attachment rate did not rise markedly, still did not overcome a 10% level. To tweak the system, a plastic cross was placed onto the membrane. It provided an additional border where ticks prefer to attach. Nevertheless, the desired outcome was not obtained. Even though the attachment rate slightly increased, the survival rate remained close to 0%.

The system for nymphal *in-vitro* feeding has been optimizing. Unfortunately, the efforts are so far of little avail. Neither of attempts to tweak the *in-vitro* feeding system have brought the highly-anticipated results. To further utilize this methodology for investigations of important tick-pathogen interactions, the whole feeding system have to be customized for nymphal ticks feeding, since ticks in a nymphal stage are the most common transmitters of Lyme disease. Empirical observation of the whole *in-vitro* feeding procedure has brought us to conclusion that preconditioning of ticks, more than any substantial changes in the membrane properties, may lead to successful employment of the silicone-membrane based *in-vitro* feeding system into nymphal tick-pathogen studies. This technique holds potential to

become a first method, which would produce nymphal ticks with almost absolute certainty of borrelial infection.

6.2 *Borrelia* plasmid content and dissemination ability

The bottom line of our study was to investigate the potential ability of *B. burgdorferi* sensu stricto spirochetes to traverse the tick gut and traffic directly to the salivary glands during a single tick feeding on an infected host. Our motivation has come partly after reading an article from Joseph Piesman *et al*. (1987). In short, they investigated time intervals needed for infected nymphs to infect rodents. They found out that *B. burgdorferi* spirochetes were transmitted to 1 of 14 rodents exposed for 24 hr, 5 of 14 rodents exposed for 48 hr, and 13 of 14 rodents exposed for 72 hr or more. This study considerably challenges the contemporary view on transmission dynamics, which highlight the importance of the preparatory phase of spirochetes in the tick gut and practically exclude the possibility that infection can occur in less than 72 hr (e.g. Dunham-Ems *et al*., 2009). Therefore, we have decided to further probe the significance of the 'in-gut' phase. We have addressed another pillar of the transmission process of *Borrelia*, which says that during the first feeding of a tick on an infected host, *B. burgdorferi* spirochetes reach solely the gut of a tick, only after second feeding on different host, the bacteria disseminate into the tick salivary glands and further to a new host.

To confirm the presence of spirochetes within the salivary glands, confocal microscopy investigation was performed. Our examinations revealed, quite unexpectedly, that *B. burgdorferi* is really able, depending on the plasmid content, to traverse the membrane of the tick gut and traffic directly to the salivary glands during a single tick feeding. It turned out that the decisive factor that probably undermined the propagation of high-passage *B. burgdorferi* was the lack of lp25. The unquestionable drawback of our study resides in fact that we compared two different *B. burgdorferi* strains; high-passage B31 and low-passage ZS7. The reason behind is that low-passage *B.burgdorferi* B31 were not available that time. We are going to perform the experiment with low-passage *B.burgdorferi* B31 in the near future. Then it will be possible to compare more reliably the passage-dependence (i.e. plasmid-dependence) of *Borrelia* on the dissemination ability, furthermore, to compare low-passage *B.burgdorferi* B31 and ZS7 for the very same aptitude. In case low-passage *B.burgdorferi* B31 with complete plasmid profile will not reach the tick salivary glands, it

may signify that another auxiliary plasmid-independent mechanism may contribute to the dissemination process, as proposed by McDowell *et al.* (2001).

The first *Borrelia* individuals (low-passage *B. burgdorferi* ZS7) were observed on the salivary glands 48 hr after attachment, in amounts not greater than 30 spirochetes per salivary gland. The bacteria were present exclusively on the acinar surface and on/in the salivary ducts, not yet inside the acini. The 48-hour time frame nicely corresponds to results obtained by Ohnishi *et al*. (2001), who observed that the route from the tick gut up to the mammalian host lasts at least 53 hr. Our findings are also in good accord with results achieved by Dunham-Ems *et al*. (2009), who documented that the vast majority of *Borrelia* escapes from the gut in a highly organized manner, not early than 48 hr after attachment. Interestingly, this would suggest that *Borrelia* need only ~5 hr to breach the membrane of the salivary glands and reach the host. It implies that *Borrelia* are extremely well adept at overcoming the acinar barrier.

It is important to note that the spirochetes were not observed within all the examined salivary glands. We estimate that *Borrelia* were localized in about one third of ticks (about 40 ticks were examined). Surprisingly, the number of spirochetes did not seem to increase during next 24 hr of feeding (i.e. 72-hour time point). It suggests that only a handful of aberrant individuals is able to reach the salivary glands, and the overwhelming majority of spirochetes stays confined to the tick gut.

A chance that *Borrelia* got into the salivary glands in other way than blood-gut-hemocoel-salivary glands can be reliably excluded. Isolation of the organs was performed very carefully with multiple washing steps, therefore, the probability that the salivary glands were tainted by spirochetes from an impaired tick gut is minimal. Additionally, the bacteria could not reach the salivary glands directly from the tick mouthpart (i.e. blood-salivary glands route), because *Borrelia* were localized on the acinar surface, furthermore, there would be no difference in spirochete numbers between low- and high-passage *Borrelia* in the salivary glands.

In order to elucidate in detail the interactions between spirochetes and *Ixodes ricinus* tissues (salivary glands), we employed another non-dynamic visualization technique - scanning electron microscopy. SEM is a method that would allow us to scrutinize the salivary gland-*Borrelia* interface. However, right after first attempts it became apparent that pursuing

Borrelia by using SEM is a process akin to searching for the proverbial needle in a haystack. The numbers of organisms within the salivary glands were minuscule, furthermore, the non-labeled spirochetes would be barely discernible from the surrounding tissue.

To cope with the lack of resolution of fluorescence microscopy and with the difficulty of *Borrelia* localization by using electron microscopy, the potential application of correlative light electron microscopy in pathogen detection has been tested. CLEM is a cutting-edge approach, which same as other new techniques, lack (almost) any kind of standardized protocols. Albeit we have surpassed many obstacles in the way to unanimous localization of *Borrelia* by CLEM, we have not been able to bring our effort to a successful conclusion. The greatest difficulties were caused by autofluorescence in the chitinous structures of the gland acini and by non-specific binding of antibodies. We have decided to address these obstructions by using *Borrelia* with stably integrated RFP (red fluorescent protein) reporter (prepared by Ryan Rego). Our study will continue as soon as the cloned *Borrelia* are ready.

The transstadial transmission of *Borrelia burgdorferi* inside the *Ixodes ricinus* salivary glands is considered to be impossible because of the glands degeneration during the molt. We have decided to conduct a cursory investigation to find out, whether the salivary glands really degenerate to such an extent, which decidedly excludes the possibilty of this phenomenom. We observed the salivary glands of the ticks in the early-molting phase, as well as of the ticks in the advanced-molting phase. Light microscopy observation and DAPI staining of the glands in the advanced-molting phase indicated that all three types (denoted I, II, III) of acini were present. This finding definitely does not exclude the possibility of the transstadial transmission of the bacteria inside the salivary glands. Of course, the question is whether the type II and III acini were present during the entire molt (i.e. did not completely degenerate), or whether these are already newly developed acini. To find the answer, the examination of the salivary glands has to be conducted throughout the molt in regular time intervals.

During the search for the salivary glands in the dissected ticks, we decided to also document the visually appealing internal morphology of the molting *I. ricinus* nymphs. The goal of this operation was not bigger than to give interesting insights into what actually happens under the cuticle (see Figures 17 and 18 in Appendix).

7 CONCLUSION

- *In-vitro* silicone membrane feeding method was successfully optimized and applied to adult ticks *Ixodes ricinus*.
- Conventional viewpoint that *B. burgdorferi* can disseminate to the salivary glands only during “second“ feeding was challenged.
- Dissemination ability of *B. burgdorferi* and their plasmid content were correlated. Linear plasmid lp25 seems to be the reason of different propagation ability of low-passage *B. burgdorferi* ZS7 and high-passage *B. burgdorferi* B31.
- Correlative light scanning electron microscopy has been tested and optimized so it can be further used in our research. To the best of our knowledge, this state-of-art technique has not been used in any other laboratory yet.
- New insights were brought into the molting process of nymphal ticks and the possibility of transstadial transmission of *Borrelia* inside the salivary glands was probed.

REFERENCES

1. Abbe, E. (1873) Beiträge zur Theorie des Mikroskops und der mikroskopischen Wahrnehmung. *Archiv für Mikroskopische Anatomie* 9, 413-418.

2. Amoreaux, W. J., Junaid, L. and Trevidi, S. (2003) Morphological evidence that salivary gland degeneration in the American dog tick, *Dermacentor variabilis* (Say), involves programmed cell death. *Tissue Cell* 35(2), 95-99.

3. Anguita, J., Ramamoorthi, N., Hovius, J. W., *et al*. (2002) Salp15, an *Ixodes scapularis* salivary protein, inhibits CD4(+) T cell activation. *Immunity* 16(6), 849-859.

4. Bacon, R. M., Kugeler, K. J. and Mead, P. S. (2008) Surveillance for Lyme disease--United States, 1992-2006. *MMWR Surveill Summ* 57(10), 1-9.

5. Barbour, A. G., Tessier, S. L. and Todd, W. J. (1983) Lyme disease spirochetes and ixodid tick spirochetes share a common surface antigenic determinant defined by a monoclonal antibody. *Infect Immun* 41(2), 795-804.

6. Barbour, A. G. and Hayes, S. F. (1986) Biology of *Borrelia* species. *Microbiol Rev* 50(4), 381-400.

7. Barbour, A.G. (1988) Plasmid analysis of *Borrelia burgdorferi*, the Lyme disease agent. *J Clin Microbiol* 26(3), 475-478.

8. Benach, J. L., Coleman, J. L., Skinner, R. A., *et al*. (1987) Adult *Ixodes dammini* on rabbits: a hypothesis for the development and transmission of *Borrelia burgdorferi*. *J Infect Dis* 155(6), 1300-1306.

9. Bonnet, S., Jouglin, M., Maladrin, L., *et al*. (2007) Transstadial and transovarial persistence of *Babesia divergens* DNA in *Ixodes ricinus* ticks fed on infected blood in a new skin-feeding technique. *Parasitology* 134(Pt 2), 197-207.

10. Bowman, A. S. and Sauer, J. R. (2004) Tick salivary glands: function, physiology and future. *Parasitology* 129, S67-81.

11. Burgdorfer, W. and Pickens, E. G. (1954) A technique employing embryonated chicken eggs for the infection of argasid ticks with *Coxiella burnetii*, *Bacterium tularense*, *Leptospira icterohaemorrhagiae*, and western equine encephalitis virus. *J Infect Dis* 94(1), 84-89.

12. Burgdorfer, W., Barbour, A. G., Hayes, S. F., *et al*. (1983) Erythema chronicum migrans--a tickborne spirochetosis. *Acta Trop* 40(1), 79-83.

13. Burgdorfer, W., Hayes, S. F. and Corwin, D. (1989) Pathophysiology of the Lyme disease spirochete, *Borrelia burgdorferi*, in ixodid ticks. *Rev Infect Dis* 11 Suppl 6, 1442-1450.

14. Burkot, T. R., Piesman, J. and Wirtz, R. A. (1994) Quantitation of the *Borrelia burgdorferi* outer surface protein A in *Ixodes scapularis*: fluctuations during the tick life cycle, doubling times, and loss while feeding. *J Infect Dis* 170(4), 883-889.

15. Casjens, S., Palmer, N., van Vugt, R., *et al*. (2000) A bacterial genome in flux: the twelve linear and nine circular extrachromosomal DNAs in an infectious isolate of the me disease spirochete *Borrelia burgdorferi*. *Mol Microbiol* 35(3), 490-516.

16. Chabaud, A. G. (1950) Sur la nutrition artificelle des tiques. *Ann Parasitol* 25, 42-47.

17. Coleman, J. L., Gebbia, J. A., Piesman, J., *et al*. (1997) Plasminogen is required for efficient dissemination of *B. burgdorferi* in ticks and for enhancement of spirochetemia in mice. *Cell* 89(7), 1111-1119.

18. Cortese, K., Diaspro, A. and Tacchetti, C. (2009) Advanced correlative light/electron microscopy: Current methods and new developments using Tokuyasu cryosections. *J Histochem Cytochem* 57(12), 1103-1112.

19. Cortese, K., Vicidomini, G., Gagliani, M. C., *et al*. (2012) 3D HDO-CLEM: cellular compartment analysis by correlative light-electron microscopy on cryosection. *Methods Cell Biol* 111, 95-115.

20. Coutte, L., Botkin, D. J., Gao, L., *et al*. (2009) Detailed analysis of sequence changes occurring during *vlsE* antigenic variation in the mouse model of *Borrelia burgdorferi* infection. *PLoS Pathog* 5(2), e1000293.

21. De Silva, A. M. and Fikrig, E. (1995) Growth and migration of *Borrelia burgdorferi* in *Ixodes ticks* during blood feeding. *Am J Trop Med Hyg* 53(4), 397-404.

22. Dunham-Ems, S., Caimano, M. J., Pal, U., *et al*. (2009) Live imaging reveals a biphasic mode of dissemination of *Borrelia burgdorferi* within ticks. *J Clin Invest* 119(12), 3652-3665.

23. Dykhuizen, D. E., Brisson, D., Sandigursky, S., *et al*. (2008) The propensity of different *Borrelia burgdorferi* sensu stricto genotypes to cause disseminated infections in humans. *Am J Trop Med Hyg* 78(5), 806-810.

24. Eicken, C., Sharma, V., Klabunde, T., *et al*. (2002) Crystal structure of Lyme disease variable surface antigen VlsE of *Borrelia burgdorferi*. *J Biol Chem* 277(24), 21691-21696.

25. Estrada-Pena, A., Bouattour, A., Camicas, J. L., *et al*. (2004) Ticks of domestic animals in the Mediterranean region: a Guide to Identification of Species. *University of Zaragoza*.

26. Fikrig, E., Pal, U., Chen, M., *et al*. (2004) OspB antibody prevents *Borrelia burgdorferi* colonization of *Ixodes scapularis*. *Infect Immun* 72(3), 1755-1759.

27. Francischetti, I. M., Sá-Nunes, A., Mans, B. J., *et al*. (2009) The role of saliva in tick feeding. *Front Biosci* 14, 2051-2088.

28. Fraser, C. M., Casjens, S., Huang, W. M., *et al*. (1997) Genomic sequence of a Lyme disease spirochaete, *Borrelia burgdorferi*. *Nature* 390(6660), 580-586.

29. Friesen, K. J. and Kaufman, W. R. (2009) Salivary gland degeneration and vitellogenesis in the ixodid tick *Amblyomma hebraeum*: Surpassing a critical weight is the prerequisite and detachment from the host is the trigger. *J Insect Physiol* 55(10), 936-942.

30. Furquim, K. C., Bechara, G. H. and Camargo Mathias, M. I. (2008) Degeneration of salivary glands of males of the tick *Rhipicephalus sanguineus* (Latreille, 1806) (Acari, *Ixodidae*). *Vet Parasitol* 154(3-4), 325-335.

31. Ge, Y., Old, I. G., Saint Girons, I., *et al*. (1997) Molecular characterization of a large *Borrelia burgdorferi* motility operon which is initiated by a consensus sigma70 promoter. *J Bacteriol* 179(9), 2289-2299.

32. Giepmans, B. N. (2008) Bridging fluorescence microscopy and electron microscopy. *Histochem Cell Biol* 130(2), 211-217.Griffith, J. M. and Posthuma, G. (2002) A reliable and convenient method to store ultrathin thawed cryosections prior to immunolabeling. *J Histochem Cytochem* 50(1), 57-62.

33. Grimm, D., Tilly, K., Byram, R., *et al*. (2004) Outer-surface protein C of the Lyme disease spirochete: A protein induced in ticks for infection of mammals. *Proc Natl Acad Sci USA* 101(9), 3142-3147.

34. Grimm, D., Tilly, K., Bueschel, D. M., *et al*. (2005) Defining plasmids required by *Borrelia burgdorferi* for colonization of tick vector *Ixodes scapularis* (Acari: *Ixodidae*). *J Med Entomol* 42(4), 676-684.

35. Gustafsson, M. G. L. (2008) Super-resolution light microscopy goes live. *Nature Methods* 5, 385-387.

36. Hadebank, B. and Hiepe, T. (1993) In-vitro-Fütterung von Zecken, *Dermacentor nuttalli*, Olenev 1928 (Acari: *Ixodidae*) über eine Silikonmembran. *Dermatol Monatsschr* 179, 292-295.

37. Hagman, K. E., Lahdenne, P., Popova, T. G., *et al*. (1998) Decorin-binding protein of *Borrelia burgdorferi* is encoded within a two-gene operon and is protective in the murine model of Lyme borreliosis. *Infect Immun* 66(6), 2674-2683.

38. Hatta, T., Miyoshi, T., Matsubayashi, M., *et al*. (2012) Semi-artificial mouse skin membrane feeding technique for adult tick, *Haemaphysalis longicornis*. *Parasit Vectors* 5, 263.

39. Hoogstraal, H. (1985) Argasid and nuttalliellid ticks as parasites and vectors. *Adv Parasitol* 24, 135-238.

40. Hovius, J. W., van Dam, A. P. and Fikrig, E. (2007) Tick-host-pathogen interactions in Lyme borreliosis. *Trends Parasitol* 23(9), 434-8.

41. Hovius, J. W., Schuijt, T. J., de Groot, K. A., *et al*. (2008) Preferential protection of *Borrelia burgdorferi* sensu stricto by a Salp15 homologue in *Ixodes ricinus* saliva. *J Infect Dis* 198(8), 1189-1197.

42. Jewett, M. W., Lawrence, K., Bestor, A. C., *et al*. (2007) The critical role of the linear plasmid lp36 in the infectious cycle of *Borrelia burgdorferi*. *Mol Microbiol* 64(5), 1358-1374.

43. Kaufman, W. R. and Lomas, L. O. (1996) “Male factors” in ticks: their role in feeding and egg development. *Invert Reprod Develop* 30(1-3), 191-198.

44. Kemp, D. H., Koudstaal, D., Roberts, J.A., *et al.* (1975) Feeding of *Boophilus microplus* larvae on a partially defned medium through thin slices of cattle skin. *Parasitology* 70(2), 243-254.

45. Kimsey, R. B. and Spielman, A. (1990) Motility of Lyme disease spirochetes in fluids as viscous as the extracellular matrix. *J Infect Dis* 162(5), 1205-1208.

46. Kolotuev, I., Schwab, Y. and Labouesse, M. (2009) A precise and rapid mapping protocol for correlative light and electron microscopy of small invertebrate organisms. *Biol Cell* 102(2), 121-132.

47. Kopáček, P., Hajdušek, O., Burešová, V., *et al*. (2010) *Tick innate immunity* 708, 137-162.

48. Kröber, T. and Guerin, P. M. (2007a) In vitro feeding assays for hard ticks. *Trends Parasitol* 23(9), 445-449.

49. Kröber, T. and Guerin, P. M. (2007b) An in vitro feeding assay to test acaricides for control of hard ticks. *Pesr Manag Sci* 63(1), 17-22.

50. Kröber, T. and Guerin, P. M. (2007c) The tick blood meal: from a living animal or from a silicone membrane? *ALTEX* 24, 39-41.

51. Kuhnert, F., Diehl, P. A. and Guerin, P. M. (1995) The life-cycle of the bont tick *Amblyomma hebraeum* in vitro. 25(8), 887-896.

52. Labandeira-Rey, M. and Skare, J. T. (2001) Decreased infectivity in *Borrelia burgdorferi* strain B31 is associated with loss of linear plasmid 25 or 28-1. *Infect Immun* 69(1), 446-455.

53. Labandeira-Rey, M., Seshu, J. and Skare, J. T. (2003) The absence of linear plasmid 25 or 28-1 of *Borrelia burgdorferi* dramatically alters the kinetics of experimental infection via distinct mechanisms. *Infect Immun* 71(8), 4608-4613.

54. Lane, R. S. and Burgdorfer, W. (1987) Transovarial and transstadial passage of *Borrelia burgdorferi* in the western black-legged tick, *Ixodes pacificus* (Acari: *Ixodidae*). *Am J Trop Med Hyg* 37(1), 188-192.

55. Li, X., Neelakanta, G., Liu, X., *et al.* (2007) Role of outer surface protein D in the *Borrelia burgdorferi* life cycle. *Infect Immun* 75(9), 4237-4244.

56. Liang, F. T., Jacobs, M. B., Bowers, L. C., *et al*. (2002) An immune evasion mechanism for spirochetal persistence in Lyme borreliosis. *J Exp Med* 195(4), 415-422.

57. Liou, W., Geuze, H. J. and Slot, J. W. (1996) Improving structural integrity of cryosections for immunogold labeling. *Histochem Cell Biol* 106(1), 41-58.

58. Lomas, L. O., Gelman, D. and Kaufman, W. R. (1998) Ecdysteroid regulation of salivary gland degeneration in the ixodid tick, *Amblyomma hebraeum*: a reconciliation of *in vivo* and *in vitro* observations. *Gen Comp Endocrinol* 109(2), 200-211.

59. Masters, B. R. (2009) History of the electron microscope in cell biology. *Encyclopedia of life sciences*, John Wiley & Sons.

60. McDowell, J. W., Sung, S. Y., Labandeira-Rey, M., *et al*. (2001) Analysis of mechanisms associated with loss of infectivity of clonal populations of *Borrelia burgdorferi* B31MI. *Infect Immun* 69(6), 3670- 3677.

61. Motaleb, M. A., Corum, L., Bono, J. L., *et al*. (2000) *Borrelia burgdorferi* periplasmic flagella have both skeletal and motility functions. *Proc Natl Acad Sci USA* 97(20), 10899–10904.

62. Narasimhan, S., Sukumaran, B., Bozdogan, U., *et al*. (2007) A tick antioxidant facilitates the Lyme disease agent's successful migration from the mammalian host to the arthropod vector. *Cell Host Microbe* 2(1), 7-18.

63. Neelakanta, G., Li, X., Pal, U., *et al*. (2007) Outer surface protein B is critical for *Borrelia burgdorferi* adherence and survival within *Ixodes* ticks. *PLoS Pathog* 3(3), e33

64. Nefedova, V. V., Korenberg, E. I., Gorelova, N. B., *et al*. (2004) Studies on the transovarial transmission of *Borrelia burgdorferi* sensu lato in the taiga tick *Ixodes persulcatus*. *Folia Parasitol (Praha)* 51(1), 67-71.

65. Norris, S. J., Howell, J. K., Garza, S. A., *et al*. (1995) High- and low-infectivity phenotypes of clonal populations of in vitro-cultured *Borrelia burgdorferi*. *Infect Immun* 63(6), 2206-2212.

66. Norstrand, A., Barbour, A. G. and Bergström, S. (2000) *Borrelia* pathogenesis research in the post-genomic and post-vaccine era. *Curr Opin Microbiol* 3(1), 86-92.

67. Ohnishi, J., Piesman, J. and De Silva, A. M. (2001) Antigenic and genetic heterogeneity of *Borrelia burgdorferi* populations transmitted by ticks. *Proc Natl Acad Sci USA* 98(2), 670-675.

68. Pal, U., Yang, X., Chen, M., *et al*. (2004a) OspC facilitates *Borrelia burgdorferi* invasion of *Ixodes scapularis* salivary glands. *J Clin Invest* 113(2), 220-230.

69. Pal, U., Li, X., Wang, T., *et al*. (2004b) TROSPA, an *Ixodes scapularis* receptor for *Borrelia burgdorferi*. *Cell* 119(4), 457-468.

70. Piesman, J., Mather, T. N., Sinsky, R. J., *et al*. (1987) Duration of tick attachment and *Borrelia burgdorferi* transmission. *J Clin Microbiol* 25(3), 557-558.

71. Piesman, J. (1995) Dispersal of the Lyme disease spirochete *Borrelia burgdorferi* to salivary glands of feeding nymphal *Ixodes scapularis* (Acari: *Ixodidae*). *J Med Entomol* 32(4), 519-521.

72. Piesman, J., Schneider, B. S. and Zeidner, N. S. (2001) Use of quantitative PCR to measure density of *Borrelia burgdorferi* in the midgut and salivary glands of feeding tick vectors. *J Clin Microbiol* 39(11), 4145-4148.

73. Powell, R. D., Halsey, C. M. and Hainfeld, J. F. (1998) Combined fluorescent and gold immunoprobes: reagents and methods for correlative light and electron microscopy. *Microsc Res Tech* 42(1), 2-12.

74. Purnell, R. E. and Joyner, L. P. (1967) Artificial feeding technique for *Rhipicephalus appendiculatus* and the transmission of *Theileria parva* from the salivary secretion. *Nature* 216, 484-485.

75. Purser, J. E. and Norris, S. J. (2000) Correlation between plasmid content and infectivity in *Borrelia burgdorferi*. *Proc Natl Acad Sci USA* 97(25), 13865-13870.

76. Purser, J. E., Lawrenz, M. B., Caimano, M. J., *et al*. (2003) A plasmid-encoded nicotinamidase (PncA) is essential for infectivity of *Borrelia burgdorferi* in a mammalian host. *Mol Microbiol* 48(3), 753-764.

77. Radolph, J. D., Caimano, M. J., Stevenson, B., *et al*. (2012) Of ticks, mice and men: understanding the dual-host lifestyle of Lyme disease spirochaetes. *Nat Rev Microbiol* 10(2), 87-99.

78. Ramamoorthi, N., Narasimhan, S., Pal, U., *et al*. (2005) The Lyme disease agent exploits a tick protein to infect the mammalian host. *Nature* 436 (7050), 573-577.

79. Rayleigh, L. (1896) On the theory of optical images, with special reference to the microscope. *Phil Mag* 42, 167-195.

80. Revel, A. T., Blevins, J. S., Almazán, C., *et al*. (2005) bptA (bbe16) is essential for the persistence of the Lyme disease spirochete, *Borrelia burgdorferi*, in its natural tick vector. *Proc Natl Acad Sci USA* 102(19), 6972-6977.

81. Rollend, L., Fish, D. and Childs, J. E. (2013) Transovarial transmission of *Borrelia* spirochetes by *Ixodes scapularis*: a summary of the literature and recent observations. *Ticks Tick Borne Dis* 4(1-2), 46-51.

82. Rudenko, N., Golovchenko, M., Grubhoffer, L., *et al*. (2011) Updates on Borrelia burgdorferi sensu lato complex with respect to public health. *Ticks Tick Borne Dis* 2(3), 123-128.

83. Samuels, D. S. and Radolph, J. D. (editors) (2010a) Ch. 6: Structure, Function and Biogenesis of the *Borrelia* Cell Envelope. *Borrelia: Molecular Biology, Host Interaction and Pathogenesis*. Caister Academic Press.

84. Samuels, D. S. and Radolph, J. D. (editors) (2010b) Ch. 2: *Borrelia* Genomics: Chromosome, Plasmids, Bacteriophages and Genetic Variation. *Borrelia: Molecular Biology, Host Interaction and Pathogenesis*. Caister Academic Press.

85. Schutzer, S. E., Fraser-Liggett, C. M., Casjens, S. R., *et al*. (2011) Whole-genome sequences of thirteen isolates of *Borrelia burgdorferi*. *J Bacteriol* 193(4), 1018-1020.

86. Schwan, T. G., Piesman, J., Golde, W. T., *et al*. (1995) Induction of an outer surface protein on *Borrelia burgdorferi* during tick feeding. *Proc Natl Acad USA* 92(7), 2909-2913.

87. Schwan, T. G. and Piesman, J. (2002) Vector interactions and molecular adaptations of Lyme disease and Relapsing fever spirochetes associated with transmission by ticks. *Emerg Infect Dis* 8(2), 115-121.

88. Schwarz, H. and Humbel, B. M. (2007) Correlative light and electron microscopy using immunolabeled resin sections. *Methods Mol Biol* 369, 229-256.

89. Serysheva, I. I., Ludtke, S. J., Baker, M. L., *et al*. (2008) Subnanometer-resolution electron cryomicroscopy-based domain models for the cytoplasmic region of skeletal muscle RyR channel. *Proc Natl Acad Sci USA* 105(28), 9610-9615.

90. Shih, C. M., Chao, L. L. and Yu, C. P. (2002) Chemotactic migration of the Lyme disease spirochete (*Borrelia burgdorferi*) to salivary gland extracts of vector ticks. *Am J Trop Med Hyg* 66(5), 616-621.

91. Singh, S. K. and Girschick, H. J. (2004) Molecular survival strategies of the Lyme disease spirochete *Borrelia burgdorferi*. *Lancet Infect Dis* 4(9), 575-583.

92. Sonenshine, D. E. and Hynes, W. L. (2008) Molecular characterization and related aspects of the innate immune response in ticks. *Front Biosci* 13, 7046-7063.

93. Sosinsky, G. E., Giepmans, B. N., Deerinck, T. J., *et al*. (2007) Markers for correlated light and electron microscopy. *Methods Cell Biol* 79, 575-591.

94. Stere, A. C., Malawista, S. E., Snydman, D.R., *et al*. (1977) Lyme arthritis: an epidemic of oligoarticular arthritis in children and adults in three Connecticut communities. *Arthritis Rheum* 20(1), 7-17.

95. Sultan, S. Z., Manne, A., Stewart, P.E., *et al*. (2013) Motility is crucial for the infectious life cycle of *Borrelia burgdorferi. Infect Immun, [*Epub ahead of print]

96. Sze, C. W., Zhang, K., Kariu, T., *et al*. (2012) *Borrelia burgdorferi* needs chemotaxis to establish infection in mammals and to accomplish its enzootic cycle. *Infect Immun* 80(7), 2485-2492.

97. Tajeri, S. and Razmi, G. R. (2011) *Hyalomma anatolicum anatolicum* and *Hyalomma dromedarii* (Acari: *Ixodidae*) imbibe bovine blood in vitro by utilizing an artificial feeding system. *Vet Parasitol* 180(3-4), 332-335.

98. Takano, A., Fujita, H., Kadosaka, T., *et al*. (2011) Characterization of reptile-associated *Borrelia* sp. in the vector tick, *Amblyomma geoemydae*, and its association with Lyme disease and relapsing fever *Borrelia* spp. *Environ Microbiol Rep* 3(5), 632-637.

99. Takano, A., Sugimori, C., Fujita, H., *et al*. (2012) A novel relapsing fever *Borrelia* sp. infects the salivary glands of the molted hard tick, *Amblyomma geoemydae*. *Ticks Tick Borne Dis* 3(4), 259-261.

100. Terekhova, D., Iyer, R., Wormser, G. P., *et al*. (2006) Comparative genome hybridization reveals substantial variation among clinical isolates of *Borrelia burgdorferi* sensu stricto with different pathogenic properties. *J Bacteriol* 188(17), 6124-6134.

101. Tilly, K., Krum, J. G., Bestor, A., *et al*. (2006) *Borrelia burgdorferi* OspC protein required exclusively in a crucial early stage of mammalian infection. *Infect Immun* 74(6), 3554-3564.

102. Tilly, K., Rosa, P. A. and Stewart, P. E. (2008) Biology of Infection with Borrelia burgdorferi. *Infect Dis Clin North Am* 22(2), 217-234.

103. Tilly, K., Bestor, A., Dulebohn, D. P., *et al*. (2009) OspC-independent infection and dissemination by host-adapted *Borrelia burgdorferi*. *Infect Immun* 77(7), 2672-2682.

104. Travinsky, B., Bunikis, J. and Barbour, A. G., *et al*. (2010) Geographic Differences in Genetic Locus Linkages for *Borrelia burgdorferi*. *Emerg Infect Dis* 16(7), 1147-1150.

105. van Dam, G. J., Bogitsh, B. J., Fransen, J. A., *et al*. (1991) Application of the FITC-anti-FITC-gold system to ultrastructural localization of antigens. *J Histochem Cytochem* 39(12), 1725-1728.

106. van Rijnsoever, C., Oorschot, V. and Klumperman, J. (2008) Correlative light-electron microscopy (CLEM) combining live-cell imaging and immunolabeling of ultrathin cryosections. *Nat Methods* 5(11), 973-980.

107. Waladde, S. M., Kemp, D. H. and Rice, M. J. (1979) Feeding electrograms and fluid uptake measurements of cattle tick *Boophilus microplus* attached on artificial membranes. *Int J Parasitol* 9(2), 89-96.

108. Wang, I. N., Dykhuizen, D. E., Qiu, W., *et al*. (1999) Genetic diversity of *ospC* in a local population of *Borrelia burgdorferi* sensu stricto. *Genetics* 151(1), 15-30.

109. Wolgemuth, C. W., Charon, N. W., Goldstein, S. F., *et al*. (2006) The flagellar cytoskeleton of the spirochetes. *J Mol Microbiol Biotechnol* 11(3-5), 221-227.

110. Wormser, G. P., Brisson, D., Liveris, D., *et al*. (2008) *Borrelia burgdorferi* genotype predicts the capacity for hematogenous dissemination during early Lyme disease. *J Infect Dis* 198(9), 1358-1364.

111. Xu, Q., Seemanapalli, S. V., McShan, K., *et al*. (2006) Constitutive expression of outer surface protein C diminishes the ability of *Borrelia burgdorferi* to evade specific humoral immunity. *Infect Immun* 74(9), 5177-5184.

112. Xu, Y., Kodner, C., Coleman, L., *et al*. (1996) Correlation of plasmids with infectivity of *Borrelia burgdorferi* sensu stricto type strain B31. *Infect Immun* 64(9), 3870-3876.

113. Yang, X., Goldberg, M. S., Popova, T. G., *et al*. (2000) Interdependence of environmental factors influencing reciprocal patterns of gene expression in virulent *Borrelia burgdorferi*. *Mol Microbiol* 37(6), 1470-1479.

114. Yang, X. F., Pal, U., Alani, S. M., *et al*. (2004) Essential role for OspA/B in the life cycle of the Lyme disease spirochete. *J Exp Med* 199(5), 641-648.

115. Zhang, J. R. and Norris, S. J. (1998) Genetic variation of the *Borrelia burgdorferi* gene *vlsE* involves cassette-specific,segmental gene conversion. *Infect Immun* 66(8), 3698-3704.

116. Zung, J. L., Lewengrub, S., Rudzinska, M. A., *et al*. (1989) Fine structural evidence for the penetration of the Lyme disease spirochete *Borrelia burgdorferi* through the gut and salivary tissues of *Ixodes dammini*. *Can J Zool* 67(7), 1737-1748.

117. FEI: Introduction to Electron Microscopy booklet, [online], <http://www.fei.com/uploadedfiles/documents/content/introduction_to_em_booklet_july_10.pdf> , downloaded 21.4. 2013

118. Speciation: Instrument Database, [online], <http://www.speciation.net/Database/Instruments/JEOL/JSM7401F-;i24>, downloaded 21.4. 2013

APPENDIX

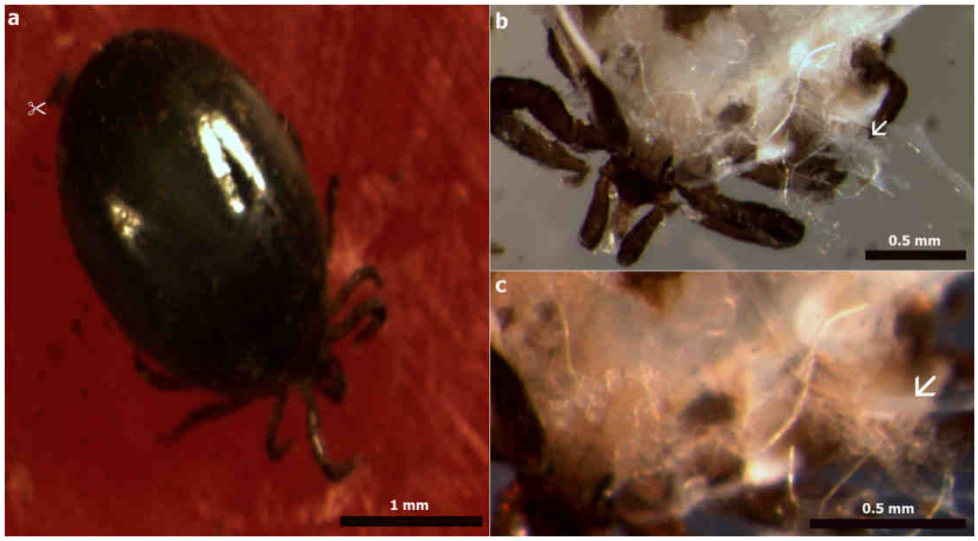

Figure 17. Examination of *I. ricinus* nymph in the early-molting phase. **(a)** The tick just before a dissection. **(b)** Internal structrure after dissection of the nymph. New cuticle is not present yet, but the salivary glands are (arrow). **(c)** A detailed image of the internal structure with the salivary glands (arrow).

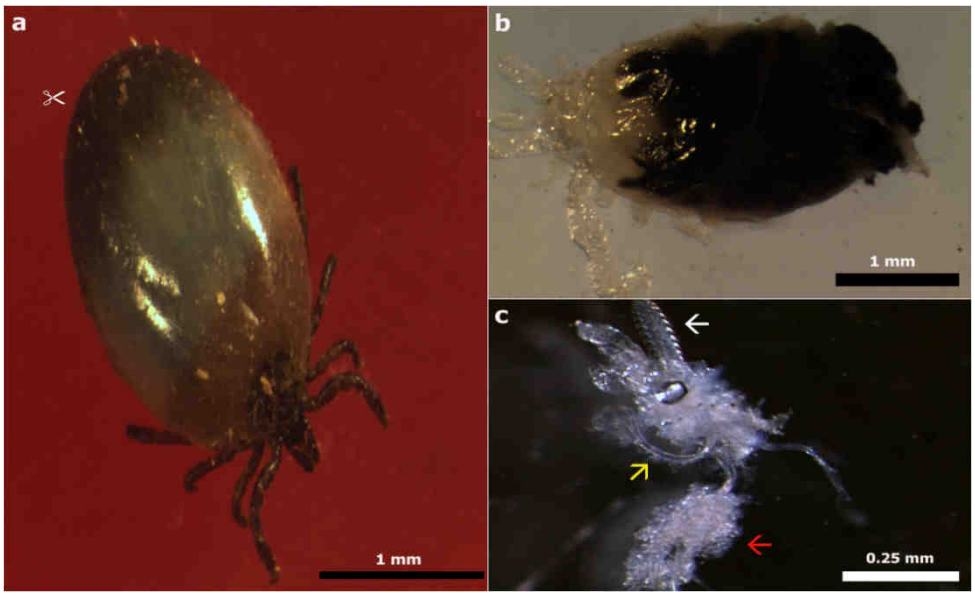

Figure 18. Examination of *I. ricinus* nymph in the advanced-molting phase. **(a)** The tick with greyish cuticle. **(b)** Internal structrure after dissection of the nymph. New cuticle was already strong enough to allow us to pull the freshly developing adult out of the old armour. **(c)** Mouthparts with a hypostome (white arrow) and a bundle of salivary glands (red arrow) connected by a salivary duct (yellow arrow).

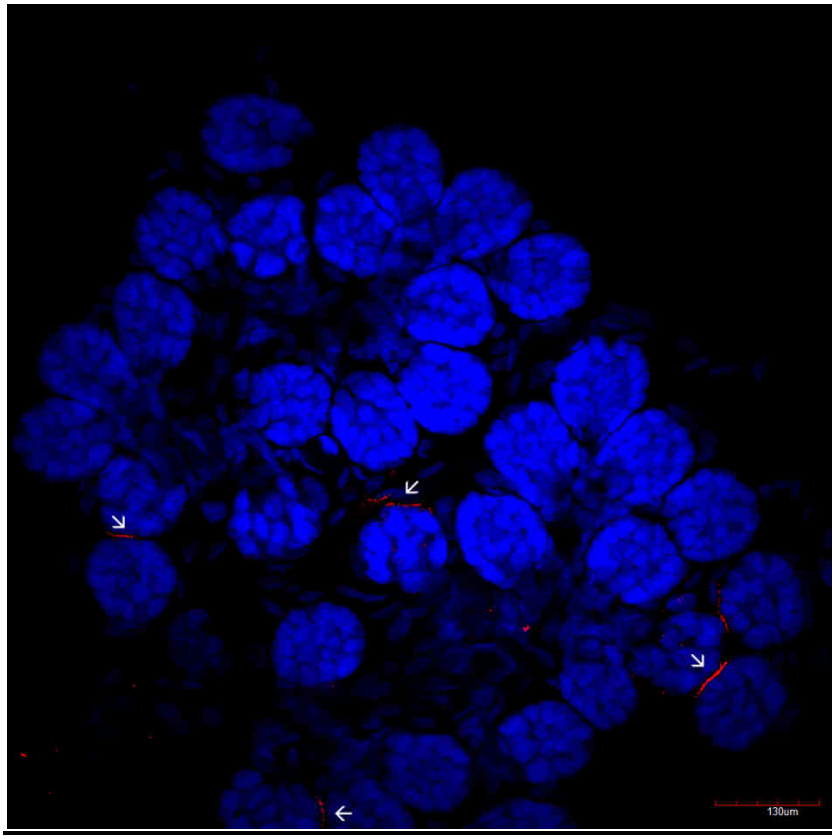

Figure 19. Salivary glands of molting *Ixodes ricinus* nymphs. Potential spirochetes (arrow) detected with rabbit anti-*B. burgdorferi* and TRITC-labeled anti-rabbit antibody. Counterstained with DAPI. Merged image.